

**NOAA NESDIS
CENTER for SATELLITE APPLICATIONS and
RESEARCH**

ALGORITHM THEORETICAL BASIS DOCUMENT

NOAA Enterprise Cloud Mask

*Andrew Heidinger, NOAA/NESDIS/STAR
William Straka, CIMSS*

Version 1.2

October 1, 2020

TABLE OF CONTENTS

1 ABSTRACT	10
2 INTRODUCTION	12
2.1 Purpose of this Document	12
2.2 Who Should Use this Document	12
2.3 Inside Each Section	12
2.4 Related Documents	12
2.5 Revision History	12
3 OBSERVING SYSTEM OVERVIEW	14
3.1 Products Generated	14
3.2 Instrument Characteristics	16
4 Algorithm Description	16
4.1 Algorithm Overview	16
4.2 Processing Outline	17
4.3 Algorithm Input	19
4.3.1 Primary Sensor Data	19
4.4 Ancillary Data	20
4.4.1 Static Ancillary Data	20
4.4.2 Dynamic Ancillary	21
4.4.3 Derived Data used in ECM	23
4.4.4 Other Derived inputs	24
5 Theoretical Description	24
5.1 Physics of the Problem	24
5.2 Use of CALIPSO Data in Determining Cloud Mask Classifiers	25
5.3 Naïve Bayesian Formulation	26
5.4 Computation of Binary Cloud Mask and Cloud Phase	27
5.5 Estimation of Uncertainty	27
5.6 Enterprise Cloud Mask Prior information	28
5.7 Selection of ECM Surface Types	30
5.7.1 DEEP OCEAN	31
5.7.2 SHALLOW WATER	31
5.7.3 LAND	31

5.7.4 SNOW	31
5.7.5 ARCTIC	31
5.7.6 ANTARCTICA	32
5.7.7 DESERT	32
5.8 Classifier Metrics	33
5.9 Optimization	37
5.10 Cloud top properties for an opaque cloud	39
5.11 Sub-pixel information for the channel	39
5.12 Uniformity Tests	40
5.12.1 Reflectance Uniformity Test (RUT)	40
5.12.2 Thermal Uniformity Test (TUT)	40
5.13 Additional Mask Algorithms	41
5.13.1 Thin Cirrus Mask	41
6 Algorithm Output	41
6.1 Cloud Probability Output	42
6.2 Cloud Mask Output	42
6.3 Single Classifier Binary Cloud Mask Bits	42
6.4 RUT and TUT	45
6.5 Metadata	45
7 Data Sets and Validation Tools	46
7.1 Input Datasets	46
7.2 Collocation	47
7.2.1 CALIPSO Data	47
7.3 Performance Metrics	48
7.4 Estimation of Specification Compliance with CALIPSO/CALIOP	50
7.4.1 VIIRS Performance Tables	50
7.4.2 ABI+AHI ECM Performance Tables	52
7.4.3 MODIS Performance Tables	53
7.5 ECM Sensitivity to Optical Depth	55
7.6 Intersensor Comparisons	57
8 Practical Considerations	59
8.1 Numerical Computation Considerations	59
8.2 Programming and Procedural Considerations	59
8.3 Quality Assessment and Diagnostics	59

8.4 Exception Handling	60
9 ASSUMPTIONS AND LIMITATIONS	61
9.1 Performance	61
9.2 Assumed Sensor Performance	61
9.2.1 Planned Product Improvements	61
9.2.2 Optimization for Land Applications	62
10 REFERENCES	62
11 Appendix A Calculation of Solar Scattering Terms	66
11.1 Rayleigh Scattering	66
11.2 Aerosol Scattering	66
11.3 Gaseous Absorption	66
11.4 Computation of Clear-sky Reflectance	67
12 Appendix B. IDL Code to Read Individual Classifier Masks	69

1 LIST OF FIGURES

Figure 1 Example of sensor input used in ECM. Images show from left to right, data location, 11 micron brightness temperature, a true color RGB and a false color RGB.

Figure 2 Main Output of the ECM. Images show posterior cloud probability, 4-level cloud mask, binary cloud mask, TUT mask and the binary cloud mask from a single classifier.

Figure 3 High Level Flowchart of the ECM illustrating the main processing sections.

Figure 4 Global total water, ice and water cloud amount for January and July derived from 9 years of monthly CALIPSO L3 data. Data in polar regions are missing in the CALIPSO data, and are derived by spatially interpolation from nearby regions.

Figure 5 Global total cloud amount for January and July derived from MODIS data.

Figure 6 The ECM surface types for January (Top) and July(bottom). Taken Heidinger et. al (2012).

Figure 7 Posterior Probabilities of a single one dimensional classifier (refrat138065) for the deep ocean surface type (SFC01). The posterior cloud probability would be 1 - posterior clear probability (black).

Figure 8 Example of a two dimensional classifier (logzopa_btd1112). The posterior cloud probability is 1 - posterior clear probability (upper right).

Figure 9 Frequency of Occurrence of Posterior Cloud Probability for each individual classifier (orange) and the final result (black).

Figure 10 Optimization example

Figure 11 Aggregated images of 8 SNPP VIIRS granules of Hurricane Andres on 06/01/2015 from 2030UTC to 2040UTC (left - True Color RGB, right - NOAA Enterprise Cloud Mask).

Figure 12 Full Disk GOES-16 ABI RGB and Binary ECM. 2020-09-20 19:00 UTC.

Figure 13 Hit Rate of the ECM as a function of CALIOP Optical Depth. ECM Lut is for VIIRS.

Figure 14 Hit Rate of the ECM as a function of CALIOP Optical Depth. ECM Lut is for ABI/AHI.

Figure 15 Hit Rate of the ECM as a function of CALIOP Optical Depth. ECM Lut is for MODIS.

2 LIST OF TABLES

Table 1 Table of ECM specifications from L1RD

Table 2 ECM focal plane temperature thresholds for GOES-17 LHP events.

Table 3 Derived Data used in the ECM.

Table 4 Description of logic for computing 4-level Mask for ECM.

Table 5 Definition of terms used in defining metrics for ECM classifiers.

Table 6 List of classifiers for the VIIRS ECM LUT and their relative importance (0=largest) for each surface type. If the cell is blank, that classifier is not on for that surface type.

Table 7 Cloud mask values and their descriptions

Table 8 Cloud mask tests and flags and their descriptions.

Table 9 Performance Metric and Cloud Fraction Comparison for the ECM compared to CALIOP. Performance Metric (PM) is ACC and clouds with optical depths less than 0.4 are ignored. TF is the truth cloud fraction from CALIOP and EF is the cloud fraction from ECM. All refers to all times of day. Day refers to daytime conditions and night refers to nighttime conditions.

Table 10 Performance Metric and Cloud Fraction Comparison for the ECM compared to CALIOP. Performance Metric (PM) is BACC and clouds with no optical depths filter TF is the truth cloud fraction from CALIOP and EF is the cloud fraction from ECM. All refers to all times of day. Day refers to daytime conditions and night refers to nighttime conditions.

Table 11 Performance Metric and Cloud Fraction Comparison for the ECM compared to CALIOP. Performance Metric (PM) is ACC and clouds with optical depths less than 0.4 are ignored. TF is the truth cloud fraction from CALIOP and EF is the cloud fraction from ECM. All refers to all times of day. Day refers to daytime conditions and night refers to nighttime conditions.

Table 12 Performance Metric and Cloud Fraction Comparison for the ECM compared to CALIOP. Performance Metric (PM) is BACC and clouds with no optical depths filter TF is the truth cloud fraction from CALIOP and EF is the cloud fraction from ECM. All refers to all times of day. Day refers to daytime conditions and night refers to nighttime conditions.

Table 13 Performance Metric and Cloud Fraction Comparison for the ECM compared to CALIOP. Performance Metric (PM) is ACC and clouds with optical depths less than 0.4 are ignored. TF is the truth cloud fraction from CALIOP and EF is the cloud fraction from ECM. All refers to all times of day. Day refers to daytime conditions and night refers to nighttime conditions.

Table 14 Performance Metric and Cloud Fraction Comparison for the ECM compared to CALIOP. Performance Metric (PM) is BACC and clouds with no optical depths filter TF is the truth cloud fraction from CALIOP and EF is the cloud fraction from ECM. All refers to all times of day. Day refers to daytime conditions and night refers to nighttime conditions.

Table 15 Performance Metric and Cloud Fraction Comparison for the NASA MYD35 compared to CALIOP. Performance Metric (PM) is BACC and clouds with no optical depths filter TF is the truth cloud fraction from CALIOP and EF is the cloud fraction from ECM. All refers to all times of day. Day refers to daytime conditions and night refers to nighttime conditions.

Table 16 Confusion matrix for SNPP VIIRS and GOES-16 ABI global colocation data for 2020-09-20 all surfaces day and night.

LIST OF ACRONYMS

1DVAR - one-dimensional variational
ABI - Advanced Baseline Imager
AIT - Algorithm Integration Team
ATBD - Algorithm Theoretical Basis Document
A-Train – Afternoon Train (Aqua, CALIPSO, CloudSat, etc.)
APOLLO – AVHRR Processing Scheme over Land, Clouds and Ocean
AVHRR - Advanced Very High Resolution Radiometer
AWG - Algorithm Working Group
CALIPSO - Cloud-Aerosol Lidar and Infrared Pathfinder Satellite
CASPR – Cloud and Surface Parameter Retrieval
CIMSS - Cooperative Institute for Meteorological Satellite Studies
CLAVR-x - Clouds from AVHRR Extended
CLAVR-1 Clouds from AVHRR Phase 1
CRTM - Community Radiative Transfer Model (CRTM)
ECM – NOAA Enterprise Cloud Mask
ECMWF - European Centre for Medium-Range Weather Forecasts
EOS - Earth Observing System
EUMETSAT- European Organization for the Exploitation of Meteorological Satellites
F&PS - Function and Performance Specification
GFS - Global Forecast System
GOES - Geostationary Operational Environmental Satellite
GOES-RRR – GOES-R Risk Reduction
IR – Infrared
IRW – IR Window
ISCCP – International Satellite Cloud Climatology Project
MODIS - Moderate Resolution Imaging Spectroradiometer
MSG - Meteosat Second Generation
NASA - National Aeronautics and Space Administration
NCEP – National Centers for Environmental Prediction
NESDIS - National Environmental Satellite, Data, and Information
NOAA - National Oceanic and Atmospheric Administration
NWP - Numerical Weather Prediction
PFAAST - Pressure layer Fast Algorithm for Atmospheric Transmittances
PLOD - Pressure Layer Optical Depth
POES - Polar Orbiting Environmental Satellite
RTM - Radiative Transfer Model
SEVIRI - Spinning Enhanced Visible and Infrared Imager
SSEC – Space Science and Engineering Center
SSM/I -- Special Sensor Microwave Imagers
STAR - Center for Satellite Applications and Research

UW – University of Wisconsin-Madison

3 ABSTRACT

The cloud detection scheme presented here is part of the suite of algorithms contained with the NOAA NESDIS Enterprise Project. It will be referred to as the NOAA Enterprise Cloud Mask (ECM). It is an evolution of the naive Bayesian cloud mask developed for the Pathfinder Atmospheres Extended (PATMOS-x) Data generated from the Advanced Very High Resolution Radiometer (AVHRR) (Heidinger et al, 2012). The ECM has evolved to support the many sensors required by the NOAA Enterprise Project. These sensors include most current and past polar orbiting and geostationary imagers.

The ECM retains many similarities to the algorithm described in Heidinger et al. (2012) including being a naive bayesian approach trained on NASA CALIPSO Data. The ECM described here has evolved to use more data from CALIPSO, support more than single-dimension classifiers and uses optimization to choose classifiers. The ECM continues to make a cloud probability and a 4-level cloud mask. The ECM also makes an ice and water cloud probability and cloud phase product. In the NOAA Enterprise System, the ECM only provides the cloud detection information. In the PATMOS-x and MODIS/VIIRS Continuity Project, the ECM also provides information on cloud phase.

This document will describe these changes and demonstrate them using the ECM applied to the data from the Advanced Baseline Image (ABI) on the GOES-16 and GOES-17 imagers, the Visible and Infrared Imaging Radiometer Suite(VIIRS), the Moderate Resolution Imaging Spectroradiometer (MODIS).

4 INTRODUCTION

4.1 Purpose of this Document

The primary purpose of this ATBD is to establish guidelines for producing the 4-level cloud mask and cloud probability from sensors flown on geostationary and polar meteorological satellites. This document will describe the required inputs, the theoretical foundation of the algorithms, the sources and magnitudes of the errors involved, practical considerations for implementation, and the assumptions and limitations associated with the product, as well as provide a high level description of the physical basis for the initial estimate of the presence or absence of cloud within each pixel. The cloud mask is made available to all subsequent algorithms that require knowledge of the presence of cloud.

4.2 Who Should Use this Document

The intended users of this document are those interested in understanding the physical basis of the algorithms and how to use the output of this algorithm to optimize the cloud detection for their particular application. This document also provides information useful to anyone maintaining or modifying the original algorithm.

4.3 Inside Each Section

This document is broken down into the following main sections.

- **System Overview:** provides a brief description of the products generated by the algorithm.
- **Algorithm Description:** provides a detailed description of the algorithm including its physical basis, its input and its output.
- **Assumptions and Limitations:** provides an overview of the current limitations of the approach and notes plans for overcoming these limitations with further algorithm development.

4.4 Related Documents

This document currently does not relate to any other document and to the references given throughout.

4.5 Revision History

Version 1.0 of this document was created by Dr. Andrew Heidinger of NOAA/NESDIS and Denis Botambekov of CIMSS/SSEC/UW-Madison. Its intent was to accompany the

delivery of the version 1.0 algorithm to the AIT NOAA Enterprise Team. In Version 1.1 several minor changes made to reflect spring 2016 ECM code delivery to AIT. In Version 1.2 a fix for Surface Type in Cloud Mask bits applied and the new BTD4_11_Day and Thin Cirrus tests were added. We also added a description of extra masks.

5 OBSERVING SYSTEM OVERVIEW

The cloud detection scheme presented here is part of the suite of algorithms contained with the NOAA NESDIS Enterprise Project. It will be referred to as the NOAA Enterprise Cloud Mask (ECM). It is an evolution of the naive Bayesian cloud mask developed for the Pathfinder Atmospheres Extended (PATMOS-x) Data generated from the Advanced Very High Resolution Radiometer (AVHRR) (Heidinger et al, 2012). The ECM has evolved to support the many sensors required by the NOAA Enterprise Project. These sensors include most current and past polar orbiting and geostationary imagers. An example of type of information used by ECM is shown in Figure 1 which shows data from SNPP VIIRS taken on June 1, 2015 at 20:30 to 20:40 UTC. Figure 1 shows (from left to right) the location of the data, an 11 micron brightness image (200-320K), a true color image and the daytime cloud type RGB constructed from the 1.38 micron (red), 0.65 micron (green) and 1.60 micron (blue) reflectances. In this RGB, cirrus are red, low water clouds are cyan, thick ice clouds are yellow and lofted water or mixed clouds are pink.

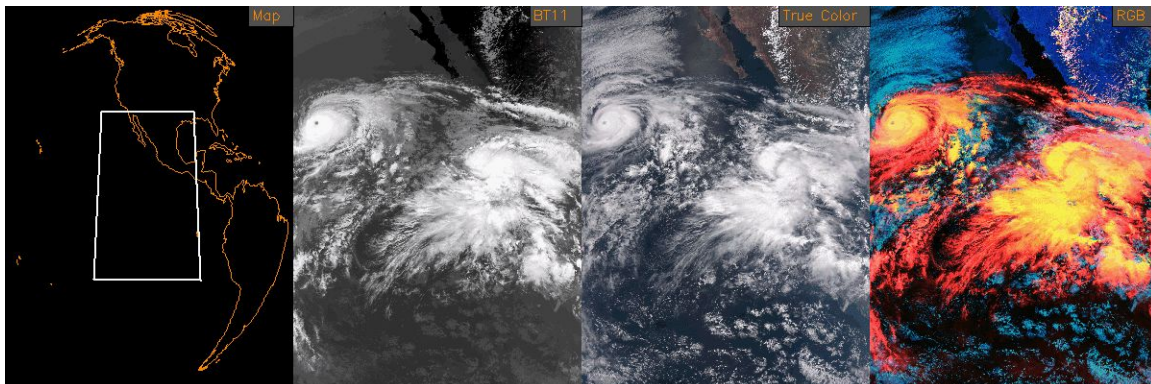


Figure 1 Example of sensor input used in ECM. Images show from left to right, data location, 11 micron brightness temperature, a true color RGB and a false color RGB.

The ECM retains many similarities to the algorithm described in Heidinger et al. (2012) including being a naive bayesian approach trained on NASA CALIPSO Data. The ECM described here has evolved to use more data from CALIPSO, support more than single-dimension classifiers and uses optimization to choose classifiers. The ECM continues to make a cloud probability and a 4-level cloud mask. The ECM also makes an ice and water cloud probability and cloud phase product. In the NOAA Enterprise System, the ECM only provides the cloud detection information. In the PATMOS-x and MODIS/VIIRS Continuity Project, the ECM does provide information on cloud phase.

The specifications for the ECM are on its probability of correct typing for the binary cloud mask. The probability of correct typing will be defined later as the accuracy (ACC) metric. The overall global ACC requirement for the ECM is 87% for clouds with an optical depth (COD) greater than 0.4. The specification also varies by surface type and illumination condition. The definition of the surface types are given later. Table 1 shows the complete ECM specifications. The section on performance measures the ECM against these specifications applied to multiple sensors and for COD > 0.4 and for no COD restrictions.

Table 1 Table of ECM specifications from L1RD

Cloud Mask Probability of Correct Typing (ACC)	Threshold Requirement
1. Global	87%
2. Ocean, Day	92%
3. Ocean, Night	90%
4. Snow-free Land, Day	90%
5. Snow-free Land, Night	88%
6. Desert, Day	85%
7. Desert, Night	85%
8. Snow-Covered Land, Day	88%
9. Snow-Covered Land, Night	85%
10. Sea-Ice, Day	82%
11. Sea-Ice, Night	72%
12. Antarctica and Greenland, Day	80%
13 Antarctica and Greenland, Night	70%

5.1 Products Generated

The cloud mask algorithm is responsible for the initial cloud detection field for all imager pixels. In terms of the JPSS Program Level 1 Requirements Document (L1RD) and L1RD SUPPLEMENT (L1RDS), it is responsible directly for the Clear Sky Mask product within the Radiance Product Category. However, the cloud mask will be used by most of the algorithms that require knowledge of the presence or absence of clouds within a given pixel. The current cloud mask requirement calls for a four-level (Confidently/Probably Clear, Confidently/Probably Cloudy) cloud mask. The ECM also generates a cloud probability from 0 to 1. The latter is considered the primary output of the ECM. In addition, the cloud mask output will include all test results that were used to determine the final four-level mask to allow for modification by downstream users.

Figure 2 presents the ECM cloud detection output for the data shown in Figure 1. From left to right, output shows the cloud probability, the 4-level mask, the binary cloud mask, the thermal uniformity test (TUT) and a binary mask from a single classifier. The single classifier, in this case, was the refrat086065 (explained later). The ECM makes a binary mask for all the classifiers used and packs into bytes for output. The TUT and the reflectance uniformity test (RUT) are not currently used in the other ECM products but they are there for users of the ECM that want to impose uniformity filters on clear pixels for their applications.

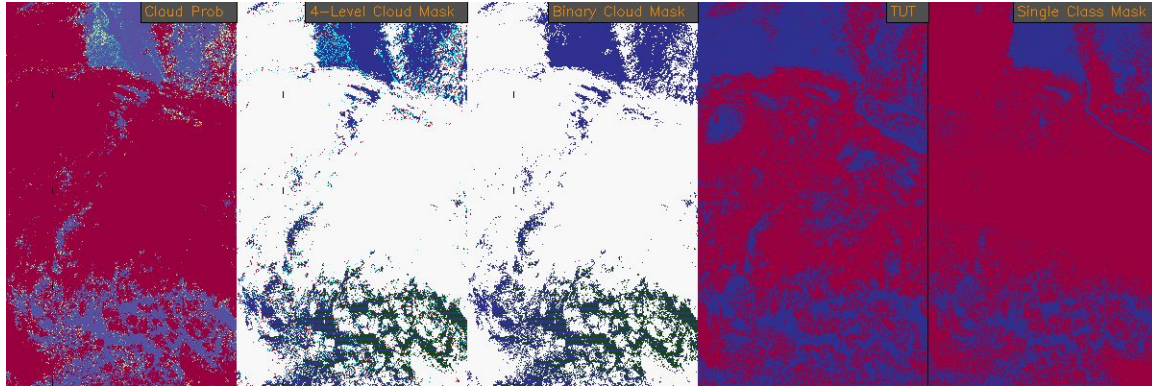


Figure 2 Main Output of the ECM. Images show posterior cloud probability, 4-level cloud mask, binary cloud mask, TUT mask and the binary cloud mask from a single classifier.

5.2 Instrument Characteristics

The cloud mask will be produced for each pixel observed by the imager sensor. The final channel set depends on sensor characteristics (band availability). The ECM is designed to work even when only a subset of the expected channels is provided. For example, when used with VIIRS data, the ECM is able to account for the lack of water vapor channels. Because the ECM also works with data from the GOES, SEVIRI, ABI, AHI, AVHRR, MODIS, etc., the exact channel combination is determined by the sensor being run and how the lookup table is generated. The only common channels among sensors are the channels associated with 0.64, 3.75, 11.0 and 12.0 μm . Some other common wavelengths that are used across more recent sensors (ex. ABI, AHI, VIIRS) include the 1.6 and 8.5 μm channels.

The algorithm relies on spectral and spatial tests, with the list of tests being provided as an attribute within the output file. The performance of the cloud mask is therefore sensitive to any imagery artifacts or instrument noise. Calibrated observations are also

critical because the cloud mask compares the observed values to those from a forward radiative transfer model. We are assuming the performance outlined in this section during our development efforts.

6 Algorithm Description

This section provides a complete description of the algorithm at the current level of maturity.

6.1 Algorithm Overview

The cloud mask serves a critical role in the Enterprise processing system. It is a fundamental cloud property in itself but also serves to determine which pixels can be used for clear-sky applications (SST, NDVI, etc.). The following heritage cloud mask algorithms have influenced the ECM:

- The MOD/MYD35 MODIS cloud mask from UW CIMSS
- The Clouds and the Earth's Radiant Energy System (CERES) MODIS cloud mask from NASA Langley Research Center
- CASPR cloud mask used in the AVHRR Polar Pathfinder Extended (APP-x)
- GOES-R Baseline Cloud Mask

As with the above masks, the ECM combines spectral and spatial tests to produce a 4-level classification of cloudiness. The 4-levels of the ECM cloud mask are:

- Clear,
- Probably Clear,
- Probably Cloudy, and
- Cloudy.

These categories are the same as those employed in the CLAVR-x and MYD35 masks. In general, the cloud mask is designed so that the clear and cloudy pixels are suitable for clear and cloudy product generation.

In addition to the 4-levels of cloudiness, the ECM also provides the results of every test used to compute the 4-level mask, and cloud probability (0.0 – 1.0). This information is provided to allow other applications to modify the cloud mask to suit their specific needs. The ordering and meaning of these bits will vary depending on the lut used. Attributes in the output files allow users to determine this information.

6.2 Processing Outline

The processing outline of the ECM is summarized in Figure 3 below. The current ECM is implemented within the Enterprise system. The Enterprise provides all of the observations and ancillary data, such as the data from NWP and RTM models. The ECM is designed to run on segments of data where a segment consists of multiple scan lines.

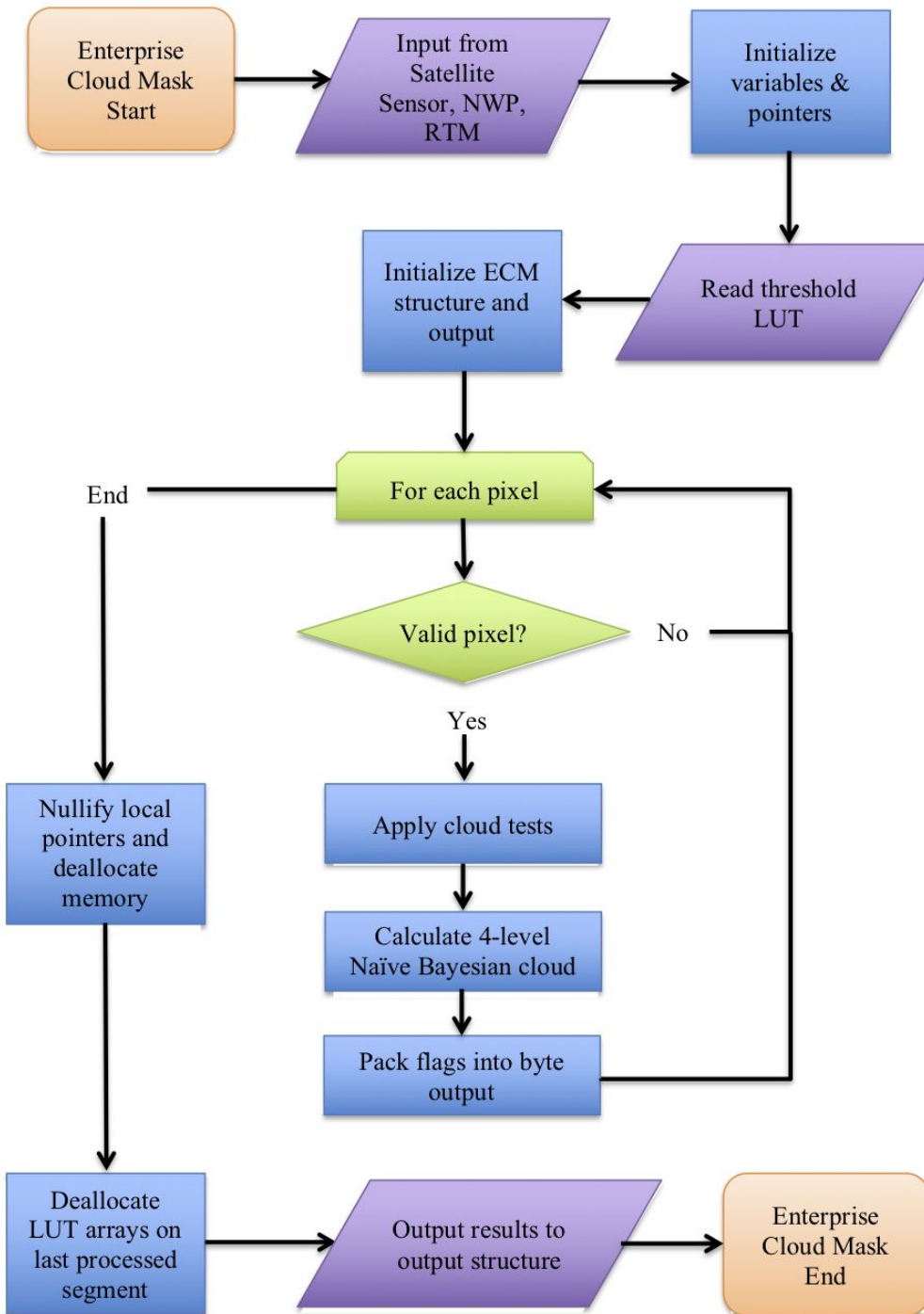


Figure 3 High Level Flowchart of the ECM illustrating the main processing sections.

6.3 Algorithm Input

This section describes the input needed to process the ECM. While the ECM is derived for each pixel, it does require knowledge of the surrounding pixels. Currently, the ECM is run on segments that contain 200 scan-lines. While the final size of the segments is to be determined, the ECM should not be run with information from only one pixel.

6.3.1 Primary Sensor Data

The list below contains the primary sensor data used by the ECM. By primary sensor data, we mean information that is derived solely from the imager sensor observations and geolocation information. The ECM uses the following available channels based on the particular sensor.

- Calibrated solar reflectance percent (0-100%) for $0.65\mu\text{m}$ (or equivalent) channel and other visible channels as needed by the LUT.
- Calibrated radiances for 3.75 , 10.3 and $11.0\ \mu\text{m}$ channels.
- Calibrated brightness temperatures for all IR channels.
 - Note - for VIIRS, the M12 band is used for the $3.75\mu\text{m}$ channel
 - Note - for ABI,AHI the Ch7 band is used for the $3.75\mu\text{m}$ channel
- Calibrated lunar reflectance percent (0-100%) VIIRS Day-Night Band (DNB).
- Bad pixel mask for each individual channel.
 - Note -The algorithm invalid mask, described in a couple sections is derived based on the channel specific quality mask
- Space mask.
- Derived $3.75\ \mu\text{m}$ channel emissivity, which is described Section 3.3.3.
- $3.75\ \mu\text{m}$ channel solar energy ($\text{mW}/\text{m}^2/\text{cm}^{-1}$).
- Sensor viewing zenith angle.

NOTE: For geostationary satellites the requirement is to produce the clear sky mask out to a sensor zenith angle of 70° .
- Solar zenith angle.
- Relative azimuth angle.
- Glint zenith angle.
- Scattering angle.
- Cosine of sensor, scattering and solar zenith angles.
- Number of lines and elements for the given segment.

● **Focal Plane Temperatures for IR and WV channels (GOES-R only)**

Mitigation for the loop heat pipe issue on GOES-17 is taken care of before the algorithm is run by checking the focal plane temperature. If either the focal plane temperature (FPT) is above the prescribed threshold, the tests for that particular

channel will not be performed and the scene will be marked as degraded via a global attribute in the GOES-R L2 file. The current temperatures allow for the ECM to be produced through the entire day, with warm events being marked as degraded. Table 2 shows the FPT thresholds utilized for each ABI channel.

Table 2 *ECM focal plane temperature thresholds for GOES-17 LHP events.*

ABI channel #	Central Wavelength (um)	Warming Side (K) Threshold	Cooling Side (K) Threshold
7	3.89	150.0	150.0
9	6.93	93.0	94.0
11	8.44	97.0	98.0
13	10.33	150.0	150.0
14	11.19	150.0	150.0
15	12.27	92.0	93.0

6.4 Ancillary Data

The following data lists the ancillary data required to run the ECM. By ancillary data, we mean data that requires information not included in the sensor observations or geolocation data. The NWP and RTM data, which are at NWP resolution, are interpolated to pixel level.

6.4.1 Static Ancillary Data

Data	Description (if necessary)
Numbers of elements, lines, maximum lines, and segments to process	
Geolocation (latitude, longitude)	
Sun earth distance	

Surface type	VIIRS Surface type or the UMD surface type as interpolated to the pixel level. Described in AIADD.
Surface Elevation	Described in AIADD. Both the surface height and standard deviation surface elevation in a 3x3 box are used in the ECM
Land Mask	MODIS Land Mask, described in AIADD
Coast Mask	Derived static coast mask, described in AIADD

6.4.2 Dynamic Ancillary

Data	Description (if necessary)
Snow Mask	Using the snow mask, each pixel is flagged internally as snow or clear. There are restoral tests for bright warm snow pixels on land. By default the ECM uses the IMS/SSMI snow mask and NWP snow mask as a backup.
Surface Emissivity 3.9, 10.3, 11 μ m	Operationally, the SEEBOR emissivity is used. However, in the future, the CAMEL emissivity database will be used
Ocean Glint Mask	A glint mask is initially defined based upon the glint zenith angle. Any non-land and snow-free pixels that have a glint zenith of less than 40° are classified as “glint.” However, those pixels that have been marked as glint and have an 11 μ m brightness temperature of less than freezing (273.15K), or the 11 μ m brightness temperature is less than the clear sky 11 μ m brightness temperature minus 5.0, have the glint flag turned off. Turning the glint mask off is an attempt to

	<p>restore cold pixels in the glint zone. Further checks are to look at pixels that have a uniform performance. A check is done by checking to see if a glint pixel has a standard deviation of $0.64\mu\text{m}$ reflectance over a 3×3 pixel array greater than 1.0. If it does, the pixel is restored to non-glint.</p> <p>At the request of the Aerosol team, after the algorithms are processed, the glint flag is set for land pixels with the glint angle less than 40 degrees</p>
Sea Surface Temperature Uniformity	Daily SST uniformity (from previous day). Operationally, the ECM uses the CMC SST output as described in the AIADD
Surface temperature from NWP	Surface temperature taken operationally from the 3,6,9 hour GFS forecasts as described in the AIADD
Surface temperature uniformity from NWP	Surface temperature taken operationally from the 3,6,9 hour GFS forecasts as described in the AIADD
Clear-sky Infrared RTM Calculations	Clear-sky top-of-atmosphere (TOA) BTs for 3.75, 6.7, 10.3 11.0 and $12.0\ \mu\text{m}$ channels. Can be used in some classifiers (ex. FMFT) if needed.
Clear-sky Reflectance	Currently the MODIS White Sky albedo is used and available for the 0.64 , 1.60 and $3.9\ \mu\text{m}$ channel. These are corrected for atmospheric scattering by adding in the Rayleigh single scattering reflectance and transmission. In the terminator region, the clear sky reflectance is renormalized.

6.4.3 Derived Data used in ECM

Table 3 lists and briefly describes the data that are required by the ECM that are provided by other algorithms or within the ECM bridge

Table 3 Derived Data used in the ECM.

Data	Description (if necessary)
Internal Valid pixel mask	A pixel is determined to be valid if it is not a space pixel, has a sensor zenith angle of less than 70°(geostationary only), and has a valid measured and clear sky 11 μ m brightness temperature.
Correlation of channel 6.9 μ m brightness temperature to channel 11.0 μ m brightness temperature	The ECM computes the Pearson Correlation Coefficient between the 6.9 and 11.0 μ m channel brightness temperatures for each pixel. For GOES-R, if the focal plane temperature is above 93.0K, this value will not be computed.
Derived top of the tropopause emissivity (ETROP)	The ECM derives the 11.0 μ m channel top of troposphere emissivity using the measured radiance, clear sky radiance, space mask, latitude/longitude cell index from the NWP, tropopause index from the NWP, viewing zenith angle bin index, and 11.0 μ m channel blackbody radiance. Currently for GOES-R, in the event that the 11 μ m focal plain temperature reaches 150K, the tropopause emissivity will be calculated using the 10.3 μ m channel.
Max/min/Standard deviation of IR resolution 0.65 μ m channel reflectance	Done over a 3x3 pixel array
Maximum 10.3 and 11.0 μ m brightness temperature	Done over a 3x3 pixel array

6.4.4 Lookup Table Description

The ECM Lookup tables (LUT) are netCDF4 files and contain the following global attributes

- sensor - the sensor that the lookup table is built for
- timestamp - the time the LUT was created
- version - the version of the lookup table
- nclassifiers - the number of classifiers
- max_length_classifier_names - the maximum number of characters for each classifier name

There are 5 variables

- classifier_names - the names of each of the classifiers. These are stored in the output (intermediate, in the case of GOES-R) file
- conf_clear_prob_clear_thresh - the cloud probability threshold between confidently clear and probably clear
- prob_clear_prob_cloud_thresh - the cloud probability threshold between probably clear and probably cloudy
- prob_cloud_conf_cloud_thresh - the cloud probability threshold between probably cloudy and confidently cloudy
- rut_clear_prob_clear_thresh - This is the thresholds for each surface that the RUT would consider a pixel probability clear
- tut_clear_prob_clear_thresh - This is the thresholds for each surface that the RUT would consider a pixel probability clear

Finally, HDF5 and NetCDF4 can organize data within the file like a file system. These are called groups. In this case, each group can store data and thresholds (variables and attributes within a given group) for a given classifier. The information for a given group within the ECM groups. There are 52 group attributes for each classifier, which consist of the name, description, information on how the classifier was made, and the thresholds for the application of the classifier (ex. angle, elevation, etc.). There are a total of 10 variables, which consist of the probability tables for each cloud type, a mask for which surfaces the classifier is applied and for which channel wavelengths the classifier is applied.

6.4.5 Other Derived inputs

The opaque cloud top properties and Sub-pixel max/min/standard deviation of reflective channels are derived within the processing system outside of the ECM and are described later.

7 Theoretical Description

Cloud detection is the process of separating cloudy from clear pixels. It always involves assumptions of the radiometric characteristics of the clear and/or cloudy state and looking

for departures from them. In the ECM, spectral, and spatial tests are used to look for clouds by identifying pixels that do not exhibit the expected behavior of the clear-sky state. Each test described is applied to each pixel, resulting in a cloud/no cloud score, which is then used to decide whether a pixel is cloudy or clear.

7.1 Physics of the Problem

The challenge for any cloud mask is to exploit spectral, spatial and temporal signatures that maximize the sensitivity to the presence of cloud while simultaneously minimizing the false detection of clouds. The ECM algorithm makes extensive use of information from NWP fields, coupled with a Radiative Transfer Model (RTM), to generate the expected clear-sky state for the spectral tests. This approach has also been adopted by EUMETSAT (Dybrro et al., 2005). While the current NWP fields often have errors in some critical fields, such as the surface temperature over land, they provide needed and useful information. Over the coming years, especially after GOES-R, NWP fields are expected to improve in both accuracy and spatial resolution. Over the coming years before the launch of GOES-R, the NWP fields are expected to improve in both accuracy and spatial resolution. For the spatial thresholds, we have no reliable information from the NWP fields and must rely on other sources. For example, the thresholds for the spatial uniformity tests rely on information from pre-computed high resolution maps of surface elevation and surface reflectance (see Section 3.3.2).

In addition, the spectral tests are broken into those that use infrared channels, shortwave infrared, and solar-reflectance channels. All applicable tests are used to construct the ECM using the Naïve Bayesian approach.

The other major type of test in the ECM is the restoral test. The restoral tests are separated into tests that “restore” probably cloudy pixels to clear pixels and tests that “restore” cloudy pixels to probably cloudy pixels. As defined, the effect of these restoral corrections is to provide a conservative estimate on cloudiness (i.e., minimize false alarms in the ECM). Note many of the cloud detection names arise from the Clouds from AVHRR (CLAVR) cloud mask developed by Stowe et al. (1999).

7.2 Use of CALIPSO Data in Determining Cloud Mask Classifiers

An important part in the development of ECM is the use of CALIPSO observations to help define the classifiers. Because CALIPSO provides one of the most unambiguous and direct measures of the presence of the highest cloud layers (i.e., those also observed by the passive sensors), it has been used to help understand the behavior of each cloud mask test for clear and cloudy pixels. While many cloud masks have used RTM simulations to set cloud detection thresholds (i.e., CASPR), the goal of the ECM is to use the availability of pixel-level clear-sky information to derive new cloud mask metrics that maximize the separation of cloudy and clear pixels. The main advantage of using an observationally based approach (collocation of CALIPSO and passive sensor test data) to

threshold definition is that simulations may not capture the true variability present in real scenes. The ECM allows for threshold modification when warranted.

In this analysis, the 1 km cloud layer product from the standard CALIPSO processing (Vaughan et al., 2005) was used together with data from the MODIS Aqua and VIIRS SNPP instruments. A key component of this analysis is the ability to co-locate the passive sensor with CALIPSO. To accomplish this, a routine was developed to find the passive sensor pixel that was closest in distance to each 1km CALIPSO cloud-layer pixel. This routine employed a nearest neighbor approach coupled with a polynomial fit to provide initial estimates of collocated pixels. The CALIPSO product, developed by NASA Langley, provides top, base and number of cloud layers for up to 10 layers in a 1 km footprint, and attempts to distinguish cloud from aerosol, smoke and dust. For the purposes of this study, a cloud mask from CALIPSO was determined noting the number of cloud layers in each 1 km pixel (column). Any CALIPSO column with more than zero cloud layers was assigned to the cloudy category. In addition, a cloud fraction from CALIPSO was computed using results from all lidar fields of view that fell within each MODIS/VIIRS pixel. Using the method described in Heidinger and Pavolonis (2009), the temperature of the highest cloud layer is used in conjunction with the 11 μm clear radiance calculation and 11 μm MODIS/VIIRS observations to compute an 11 μm cloud emissivity. This value represents the emissivity that a cloud must have if it existed at the level measured by CALIPSO with the observations measured by the passive sensor (i.e., SEVIRI, VIIRS, MODIS, etc.). This is hereafter referred to as the CALIPSO emissivity.

As a lidar with an inherent vertical resolution of 30 m, CALIPSO can detect clouds with opacities and spatial scales far exceeding the capabilities of passive visible/infrared sensors such as MODIS or the VIIRS. In order to use CALIPSO to determine meaningful thresholds for passive detection of clear and cloudy conditions, filtering is required to attempt to make the CALIPSO detection comparable to the performance expected from the passive observing system. In this analysis, we ignored all CALIPSO results which had cloud fractions not equal to 0.1 or 1.0. The purpose of this filter is to restrict the analysis to CALIPSO data that is uniform over the spatial scales of the coarser MODIS or VIIRS pixels. In addition, a threshold of 0.1 was applied to the CALIPSO emissivity in an attempt to remove from consideration any pixels with very low optical depths that would fall below the detection capabilities of the channels on the passive sensors.

In the remaining part of this section, CALIPSO data matched in space and time with MODIS or VIIRS observations are used to demonstrate the skill of the cloud mask tests in the ECM.

7.3 Naïve Bayesian Formulation

The naive Bayesian formulation used here is the same as described in Heidinger et al. (2012). One simplification is employed. The formulation requires the calculation of class conditional no and yes values. These represent the fraction of all yes (or no) within a bin compared to the total number of yes (or no) in all bins. The class conditional no and yes values are ratioed and multiplied together to form the variable R as shown below,

$$R = \prod_i^n \frac{C_{no,i}}{C_{yes,i}}$$

he calculation of the posterior probability P_p simplifies to the following

$$P_p = \frac{1}{1 + \frac{P_r}{R}}$$

Where P_r is the prior probability. In addition to the algebraic simplicity, this change allows the lookup tables to store only the ratio of the yes and no class conditional values, not both of them.

Previous versions of the ECM used the CALIOP Cloud Phase values to generate a binary cloud mask and the ECM only generated the probability of cloud. This version of ECM now uses ice and water information in the CALIOP cloud phase to estimate a pixel's probability of being clear (cloud-free), ice-cloud or water-cloud. These three probabilities are accomplished in the same way.

Because the prior values used in the ECM may differ from the prior values of the training data, the 3 probabilities may not sum to 1.0. Therefore, the first step is to sum the clear, water and ice probabilities and divide each by that sum.

$$\begin{aligned} P_{sum} &= P_{clear} + P_{water} + P_{ice} \\ P_{clear} &= P_{clear} / P_{sum} \\ P_{water} &= P_{water} / P_{sum} \\ P_{ice} &= P_{ice} / P_{sum} \end{aligned}$$

$$P_{cloud} = 1 - P_{clear}$$

7.4 Computation of Binary Cloud Mask and Cloud Phase

This section describes how the posterior probabilities from the ECM are converted into the binary cloud mask and the cloud phase. As stated above, the cloud phase is meant only to diagnose the cloud mask and is not a replacement for the Enterprise Cloud Phase product. These quantities are computed as shown in the following pseudo-code:

If $P_{\text{cloud}} < 0.50$
 Binary Cloud Mask = Clear
 Cloud Phase = Clear

If $P_{\text{cloud}} > 0.50$
 Binary Cloud Mask = Cloudy
 Cloud Phase is water if $P_{\text{water}} > P_{\text{ice}}$
 Cloud Phase is ice if $P_{\text{ice}} \geq P_{\text{water}}$

7.5 Estimation of Uncertainty

In addition to the masks, the posterior probabilities are also used to generate uncertainties in the cloud detection and cloud phase as follows.

Cloud phase uncertainty = $1.0 - P_{\text{ice}}$ or $1 - P_{\text{water}}$

Cloud Mask uncertainty = P_{cloud} if binary cloud mask is clear
 Cloud mask uncertainty = $1 - P_{\text{cloud}}$ if binary cloud mask is cloudy

7.5.1 Computation of 4-Level Cloud Mask

The ECM also makes a 4-level cloud mask. The 4-Level Cloud Mask is initialized from the binary mask. Thresholds on P_{cloud} are used to determine as shown below.

Table 4 Description of logic for computing 4-level Mask for ECM.

	Binary Mask	Pcloud	RUT (opt)	TUT (opt)
Conf Clear	Clear	0 - PCC	uni	uni
Prob Clear	Clear	PCC - 0.5	non-uni	non-uni
Prob Cloudy	Cloudy	0.5 - PCD	N/A	N/A
Conf Cloudy	Cloudy	PCD-1.0	N/A	N/A

PCC is the cloud probability threshold between the confidently and probably clear mask values and PCD is the cloud probability threshold between the probably cloudy and confidently cloudy mask values. In past versions of the ECM, PCC was set to 0.1 and Pcd was set to 0.9. These fixed thresholds resulted in a lack of confidently clear pixels. These fixed thresholds resulted in varying amounts of confidently-clear for each surface type. From a probabilistic point of view, this makes sense since the confidence in cloud

detection does vary greatly with surface and viewing conditions. However, some algorithms rely on the ECM to provide confidently clear pixels. Therefore, the ECM applies an approach that sets the PCC values to ensure that each surface type on average yields 25% of the binary-clear pixels as confidently clear. For the PCD values, the previous value of 0.9 was kept because a fixed value did not seem to cause issues to the downstream algorithms. Applying this approach to the VIIRS data gives different values for PCC for each surface.

7.6 Enterprise Cloud Mask Prior information

The posterior prior probability is derived using the CALIPSO Version 1.00 Lidar Level 3 GEWEX cloud monthly product, which is available on the Detailed Quality Summary website,

https://www-calipso.larc.nasa.gov/resources/calipso_users_guide/qs/cal_lid_l3_gewex_cloud_v1-00.php (accessed September 2020). Monthly data from 2007 to 2015 were used to compute mean and standard deviation cloud fractions for each month at $1^{\circ} \times 1^{\circ}$ box over the entire globe. These calculations are done for the total cloud amount as well as separating ice and water clouds, which are treated separately. In addition, averages for daytime, nighttime and day-night are provided in the CALIPSO L3 files. This allows for the mean and standard deviation for total, ice and water clouds can be computed for different solar illumination conditions. Due to how CALIPSO orbits, not every grid cell has a valid value every month, especially when separating day/night scenes and ice/water clouds. Under conditions when a grid cell doesn't have a valid value, a spatial averaging with a box size of $9^{\circ} \times 9^{\circ}$ is applied in order to fill those regions. Many iterations are conducted to fill all cells and are applied to grid cells that show a mean cloud amount of 1.00. This allows the posterior prior probability to look more realistic. Finally, spatial smoothing is applied to the data after all grid cells are filled. Both datasets, with and without the spatial smoothing, are within the prior cloud amount lookup table and available for use. The figure below shows the global total, ice and water cloud amount for January and July, respectively. The data plotted are not spatially smoothed. Artifacts are observed in polar regions which are due to missing values from the CALIPSO products so spatial averaging is applied as described previously.

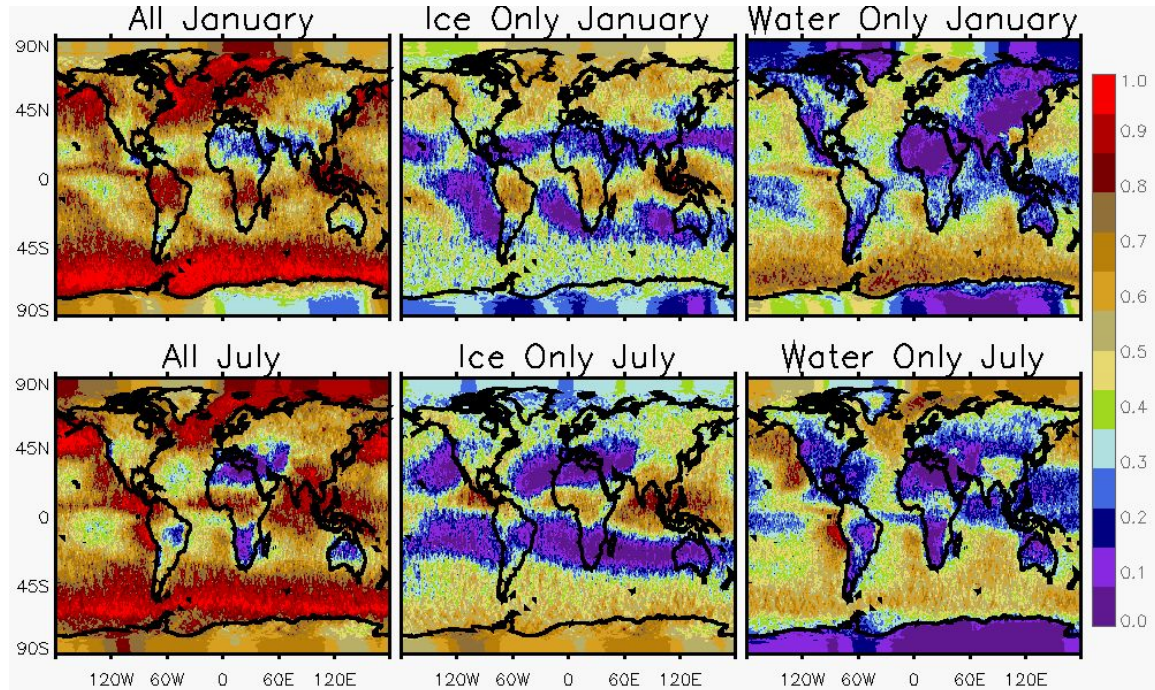


Figure 4 Global total water, ice and water cloud amount for January and July derived from 9 years of monthly CALIPSO L3 data. Data in polar regions are missing in the CALIPSO data, and are derived by spatially interpolation from nearby regions.

Previously, the ECM only used just the total cloud fraction from MODIS, derived from the MOD35 product. While the monthly data was used to compute mean and standard deviation cloud fractions for each month at $1^\circ \times 1^\circ$ box over the entire globe, there was no need to fill in any gaps in the polar regions, since the grid cells all had valid values. However, there were differences in the performance of the MODIS cloud mask owing to the usage of the visible channels during the day and the limitations of IR cloud masking over the polar regions during the nighttime region. In addition, unlike the latest CALIOP prior mask, the MODIS prior was not separated by cloud type (water/ice). Thus only the total cloud fraction was available. Similar to the image above, the figure below shows the total cloud fraction from January and July.

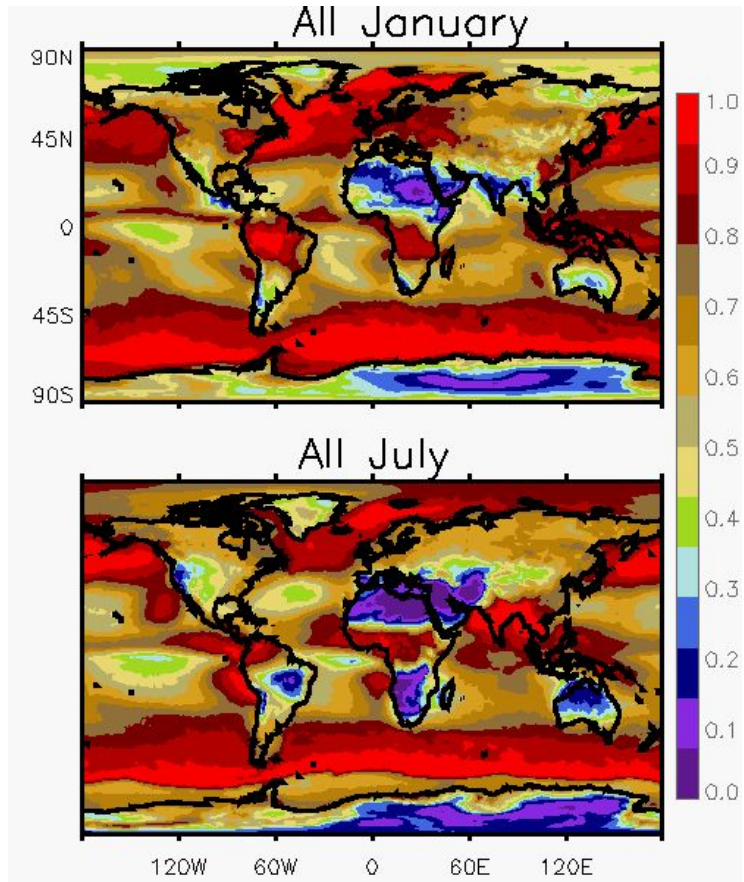


Figure 5 Global total cloud amount for January and July derived from MODIS data.

The most noticeable differences are in the polar regions, especially in the hemispheres' winter. This is mostly due to the fact that, as mentioned above, MODIS, which is an optical sensor, reverts to an IR only algorithm at night. The other difference is that MODIS is more smooth, owing to the larger footprint of the sensor.

7.7 Selection of ECM Surface Types

As stated above, the selection of different surface types to generate the classifiers is critical. We have chosen to classify the globe into seven surface types. The goal of classifying different surface types is to capture the systematic biases in our knowledge of the clear-sky conditions that vary greatly from one surface type to another. In the current algorithm, we classify the globe into the following surface types: 1-DEEP OCEAN, 2-SHALLOW WATER, 3-LAND, 4-SNOW, 5-ARCTIC, 6-ANTARCTIC, and 7-DESERT. These surface types were chosen after a series of trial and error experiments. Each surface type represents a region where the distribution in the contrast between clear and cloudy skies and the accuracy of the performance of the clear-sky

model is similar. The inputs to the surface type are the land cover data from the land cover database used in the MODIS geolocation file (MOD/MYD03), the snow field within the NCEP reanalysis (Kalnay et al, 1996), the NOAA Optimum Interpolation Sea Surface Temperature Version 2 (OISST) daily 25 km SST analysis (Reynolds et al., 2002) and 3.75 μm surface emissivity from the SEEBOR surface emissivity data base (Seeman et al, 2008). Figure 3 shows the global distribution of these surface types for January 1 and July 1, 2009. A brief description of these types follows. The surface types will vary with the frequency of the ancillary data. While the land cover data is temporally invariant, the surface emissivity values vary every 16 days. The largest driver of the surface type variation is the snow and ice cover information. The sea-ice information is taken from the OISST data and varies daily. The snow information is taken from the NCEP Reanalysis, which is updated every 6 hours.

7.7.1 DEEP OCEAN

The DEEP OCEAN surface type consists of pixels where the MOD03 land mask was set to “Deep Ocean” and the sea-ice information from the OISST data indicated ice-free conditions. Highly accurate clear-sky radiative transfer modeling and spatially uniform surfaces characterize the DEEP OCEAN surface type.

7.7.2 SHALLOW WATER

The SHALLOW WATER surface type is defined by ice-free pixels that the MOD03 land mask classified as Moderate Ocean, Deep-Inland-Water and Shallow-Inland Water. In addition, any pixels where the 3x3 standard deviation of the background SST from the OISST exceeds 1.0 K were also included in the SHALLOW WATER surface type. In general, this surface type includes water bodies where our knowledge of the surface temperature is much less accurate than that of the DEEP OCEAN surface type.

7.7.3 LAND

The LAND surface type includes all land surfaces that are not covered by snow and not classified as desert.

7.7.4 SNOW

The SNOW surface type includes all land surfaces covered by snow excluding Antarctica and Greenland.

7.7.5 ARCTIC

The ARCTIC surface type includes all pixels labeled as sea-ice in the Northern Hemisphere.

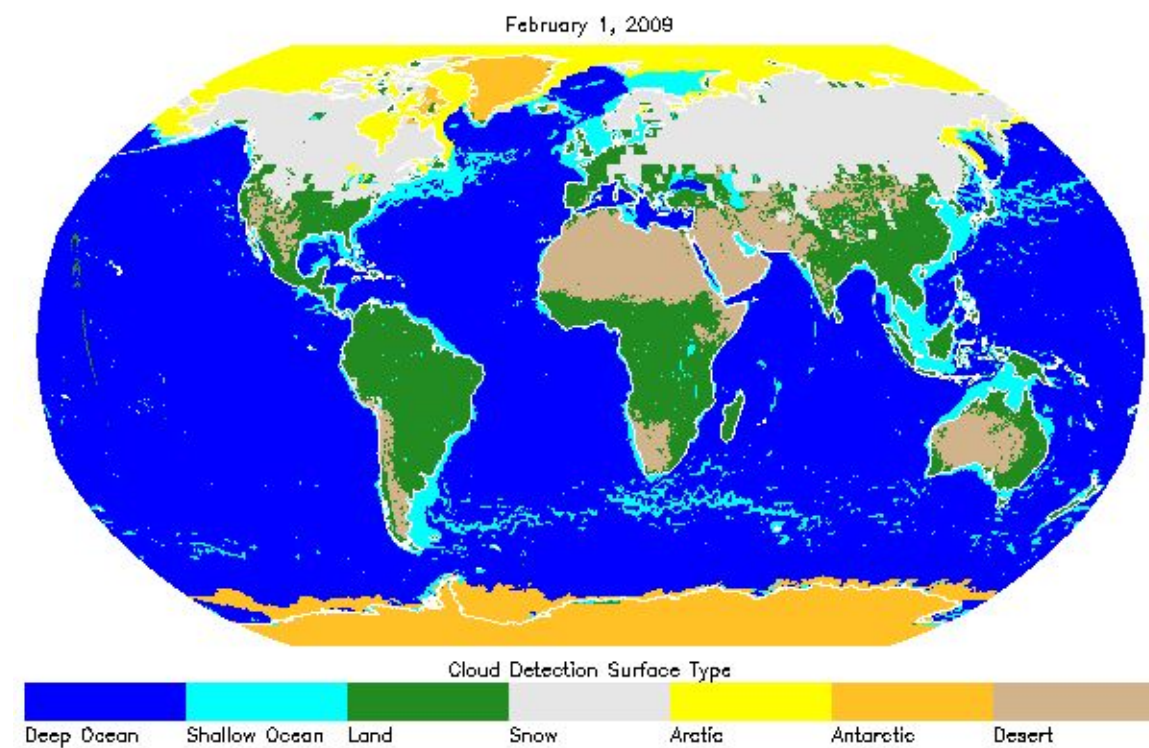
7.7.6 ANTARCTICA

The ANTARCTICA surface type includes all sea-ice in the Southern Hemisphere and all snow covered surfaces south of 60S. Based on guidance from the MODIS cloud mask team located at the University of Wisconsin, snow covered Greenland was also included in the ANTARCTICA surface type.

7.7.7 DESERT

The DESERT surface type includes all pixels with a 3.75 μm surface emissivity less than 0.90 that occurred within 60 latitudinal degrees of the equator. The use of the 3.75 μm emissivity was used to ensure optimal performance for the 3.75 μm classifiers.

Figure 6 shows the global distribution of the surface types for February 1, 2009 (top) and July 1, 2009 (bottom). As Figure 3 shows, the spatial coverage of these surface types varies with season with snow-covered land showing the most dramatic variation. The appearance of SHALLOW OCEAN away from the coasts is due to the inclusion of heterogeneous SST regions (i.e. oceanic fronts) into this surface type.



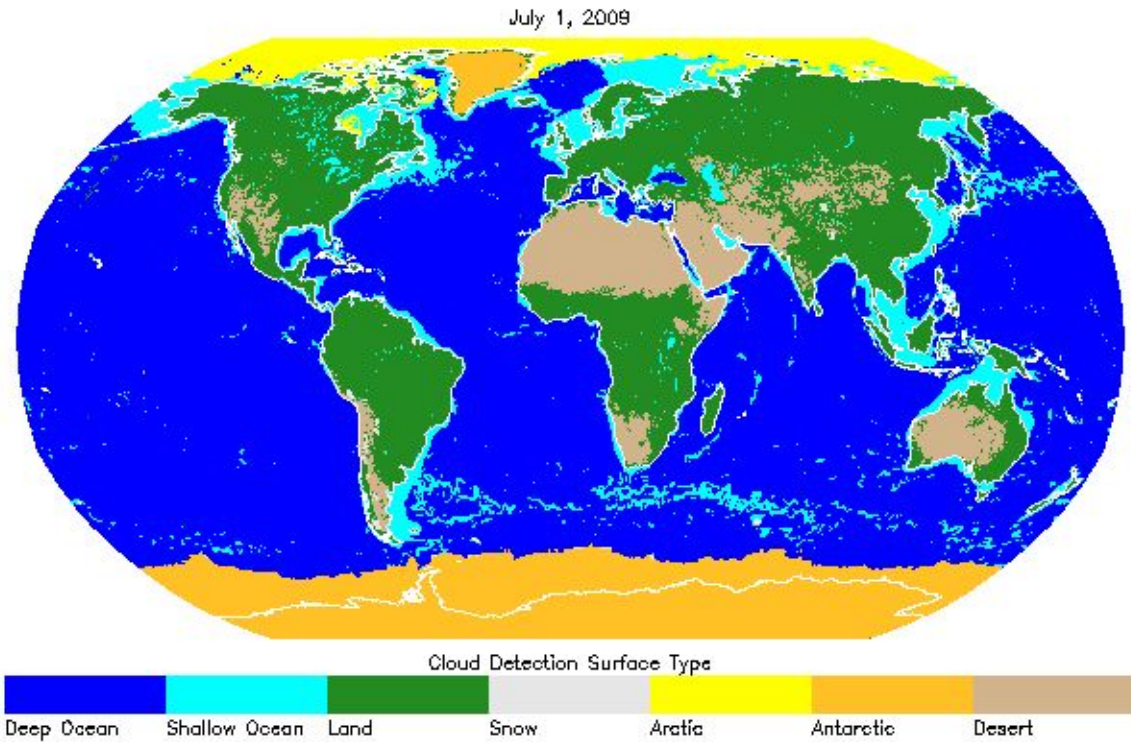


Figure 6 The ECM surface types for January (Top) and July (bottom). Taken Heidinger et al (2012).

7.8 Classifier Metrics

Given the range of sensors supported by the ECM, the number of metrics used in constructing the classifiers used in the ECM LUTs is large. The metrics can include observations, algebraic relationships of observations, clear-sky values and newly derived variables specifically made for cloud detection. The table below gives some examples of how the metrics are defined and the naming convention used. Note, this table is not meant to be complete. For example, all brightness temperatures and all standard brightness temperature values are available.

Table 5 Definition of terms used in defining metrics for ECM classifiers.

Metric Name	Definition
bt	brightness temperature (bt11 = 11 micron brightness temperature)
btd	Brightness temperature difference (btd1112 = bt11 - bt12)

std	Standard deviation of on a 3x3 array centered on the pixel
zopa	Opaque cloud height
topa	Opaque cloud temperature
dtsfcopa	Difference in surface and opaque cloud temperature
etropo	emissivity referenced to tropopause (ie etropo11 = 11 micron etropo)
ref	Reflectance (ref065 = 0.65 micron reflectance)
clr	Clear sky (ref065clr = clear sky 0.65 micron reflectance)
drefl065clr	Difference in the 0.65 reflectance with the clear-sky value
refratxy	Reflectance ratio of x /y (refrat086065 = ref086 / ref065)
xstd	Standard deviation of x over 3x3 array
logx	Log10 of x
day	Metric computed only for day defined solar zenith angle
night	Metric computed only for night defined solar zenith angle

Once the metrics for the classifiers are defined, they are used by themselves in 1d classifiers or combined with others to make 2d and 3d classifiers. As described above, each classifier can be used with the prior probabilities to make a posterior probability by itself. Examples of single classifier posterior probabilities are shown below. Figure 7 shows a single 1d refrat138065 classifier for the deep ocean surface type. This classifier is very sensitive to high clouds and can not discriminate between obscured low clouds and clear sky. Figure 7 shows the variation of the posterior probabilities for clear, ice and water clouds and also shows the frequency of the observations for each value of the classifier metric.

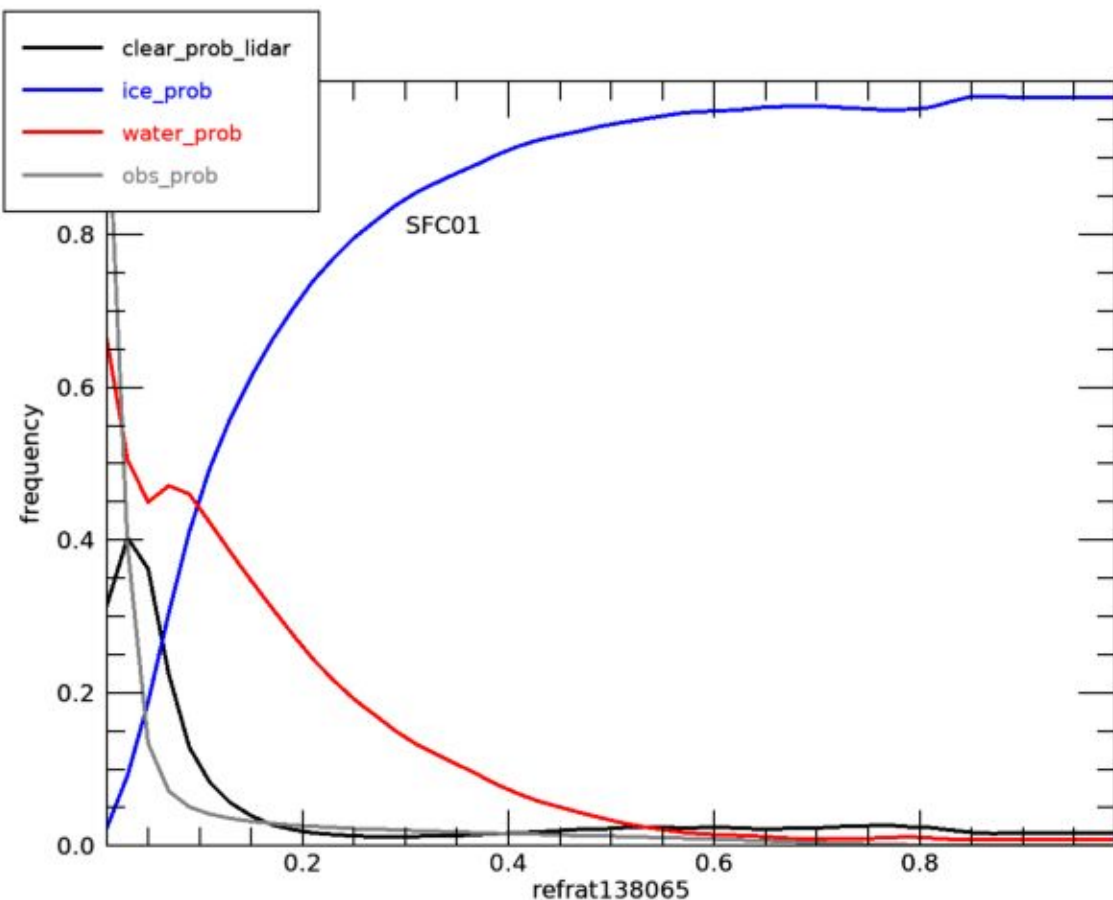


Figure 7 Posterior Probabilities of a single one dimensional classifier (refrat138065) for the deep ocean surface type (SFC01). The posterior cloud probability would be 1 - posterior clear probability (black).

Figure 8 shows the posterior probabilities for a single 2d logzopa_btd1112 classifier for the deep ocean surface type. The OBS_PROB field shows the relative location of the training data in 2d space. Red values are high probability and blue values are low probability. An ideal classifier has red regions in each field (clear, ice, and water) that do not overlap each other.

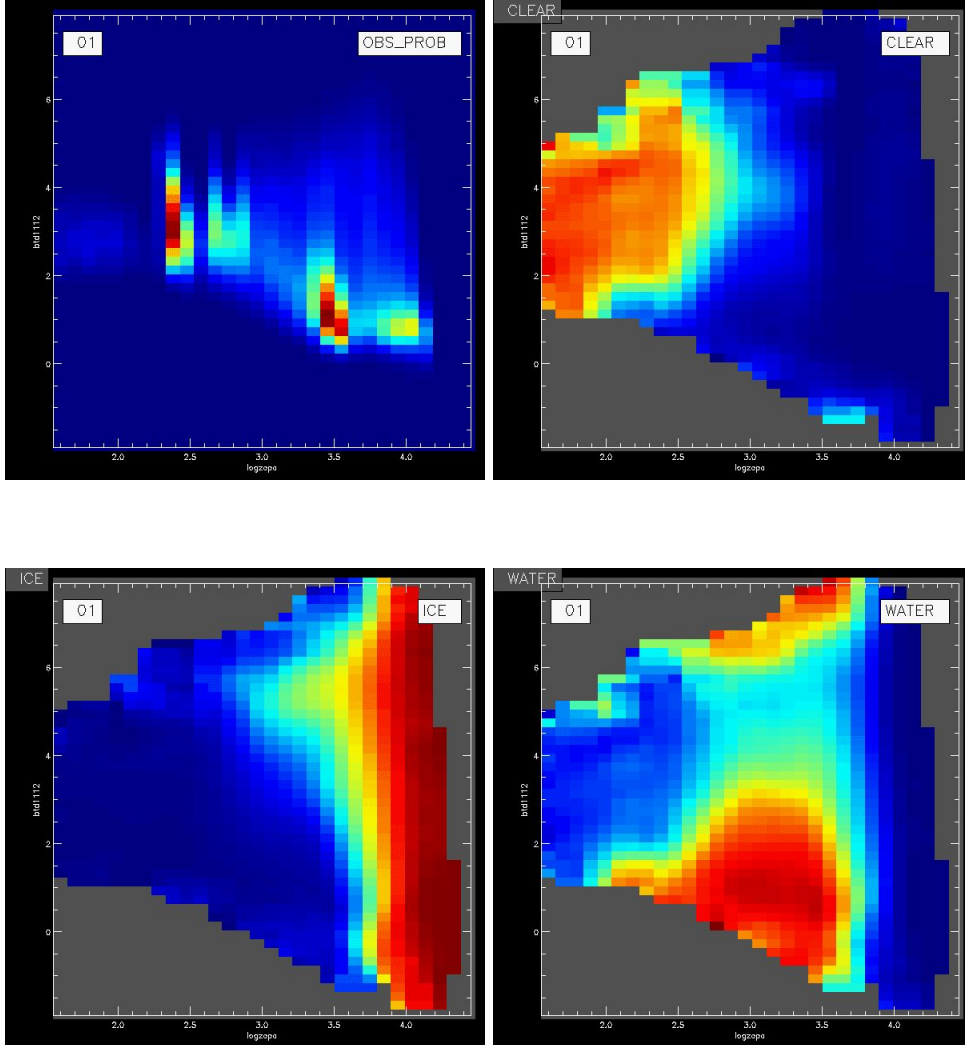


Figure 8 Example of a two dimensional classifier (logzopa_btd1112). The posterior cloud probability is 1 - posterior clear probability (upper right).

Due to the difficulty in visualization, a 3d classifier is not shown. Once all of the classifiers are made, they are combined manually or through the optimization process to make an ECM Look-up Table (LUT). The goal of combining classifiers is to get better results than from any one classifier. For the VIIRS ECM LUT described here, Figure X shows the frequency distribution of the posterior cloud probabilities from each classifier alone (orange) and from the final values from all classifiers (black). Ideal behavior would be the final frequencies to be clustered near 0 and 1. This appears to be the behavior for this LUT even none of the individual classifiers shows this behavior.

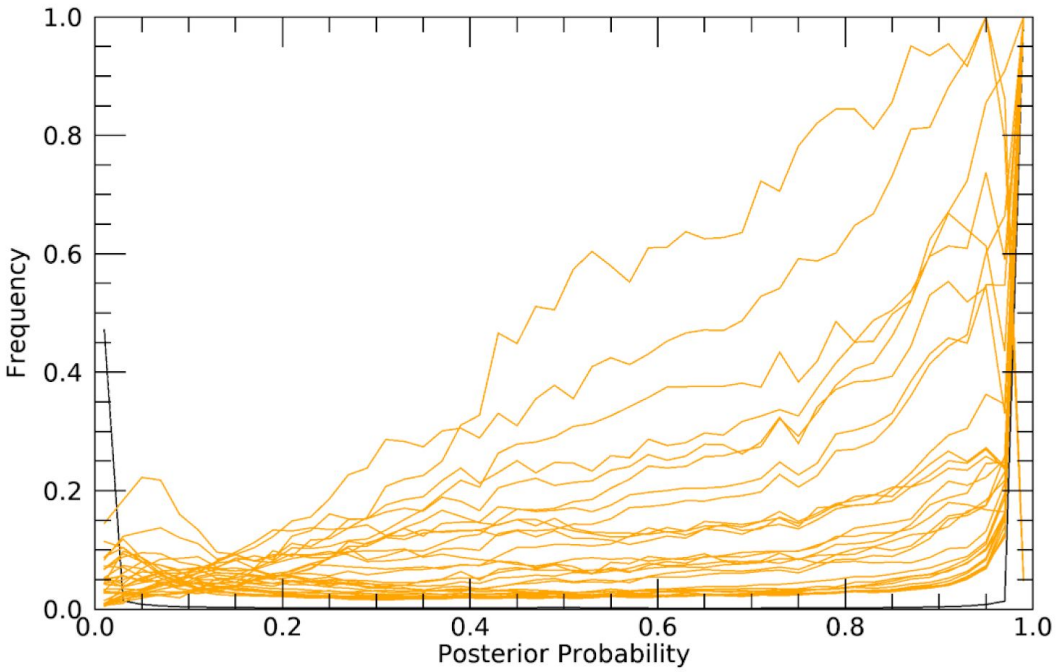


Figure 9 Frequency of Occurrence of Posterior Cloud Probability for each individual classifier (orange) and the final result (black).

7.9 Optimization

If classifiers are combined, there is a risk that correlations between the classifiers will result in a reduction in performance. To remedy this, an optimization procedure was developed. The process used is sequential optimization. The optimization is applied for each surface type or globally. The process starts by picking one of the metrics described above. The classifiers are ranked by their individual performance. The winner is saved and becomes the baseline. The process is repeated by selecting which remaining classifier improves upon the baseline the most. The best classifier is then added to the baseline and the process is repeated until the improvements to performance become negligible. This process is assumed to reduce the impact of classifier correlation.

The optimization for a set of classifiers for the snow surface is shown below. For this example, the zopa_btd1112_logbt11std classifier is the most powerful single classifier.

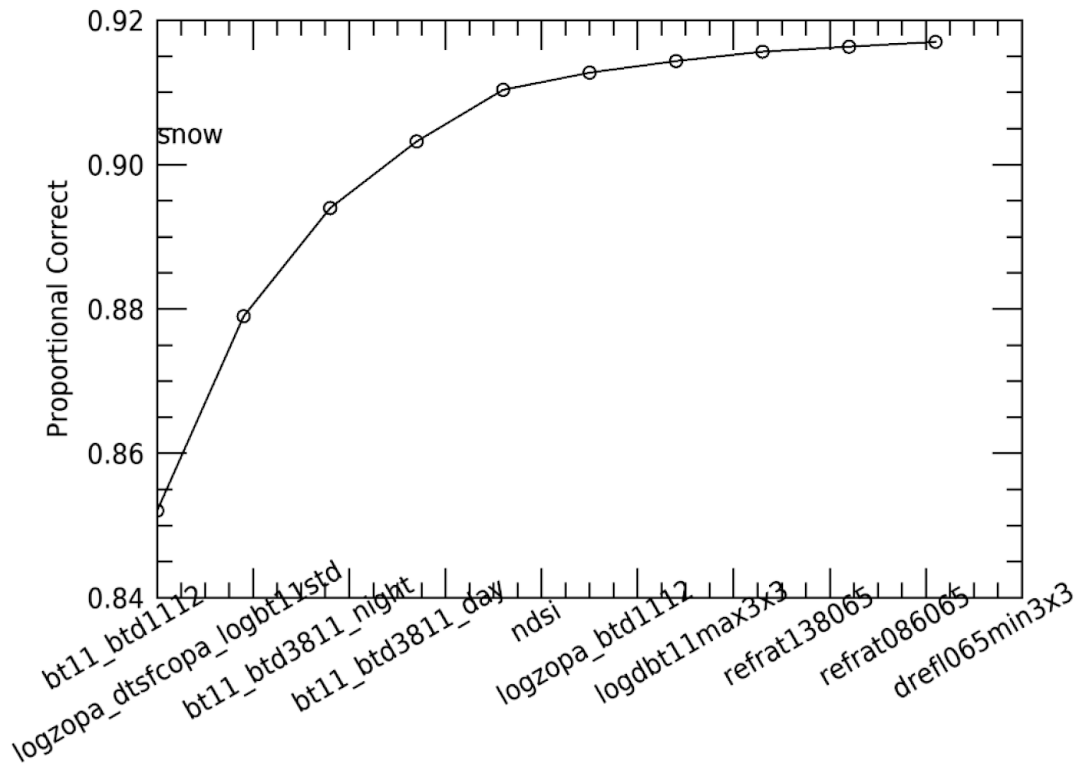


Figure 10 Optimization example

Table 6 List of classifiers for the VIIRS ECM LUT and their relative importance (0=largest) for each surface type. If the cell is blank, that classifier is not on for that surface type.

		Surface Type Index							
Class Index	Test Name	0	1	2	3	4	5	6	7
0	bt11_btd1112	2			0	2	6	5	0
1	bt11_btd3811_day	1	3		2	1	4	3	
2	bt11_btd3811_night					5	2		
3	dbt11max3x3	5	1	1	8		11		

4	drefl065min3x3	6	6	5		7	10	6	4
5	etropo11_btd1112_logbt11std	8			6		3		1
6	etropo11_dtsfcopa_logbt11std						7		
7	etropo11_logbt11std		4	0					
8	etropo11_topa_logbt11std				1		0		
9	logbt11std_logrefl065std						5		2
10	logzopa_btd1112		5	4				2	
11	logzopa_btd1112_logbt11std	4			4	0	9	0	
12	logzopa_dtsfcopa	7					12	4	
13	logzopa_dtsfcopa_logbt11std	0				4			
14	logzopa_topa_logbt11std		0						
15	ndsi	3				3	3	1	1
16	refrat086065		2	2	7				
17	refrat138065		7	3	5	6	8		3

7.10 Cloud top properties for an opaque cloud

The opaque cloud properties provide an estimate of the cloud top height, temperature and pressure based on the IR measured temperature and the RTM. It provides a basic idea of the properties of an opaque (dark) for a given pixel. The objective is to get information (height, temperature and pressure) of an opaque cloud for a given pixel and to use this information to determine the likelihood of a pixel being the cloud. To determine the level of an opaque cloud, one takes the measured $11\mu\text{m}$ (or $10.3\mu\text{m}$) radiance and then looks through the radiance profile from the RTM to determine the cloud properties. The uncertainties associated with clear-sky radiative transfer for opaque clouds are assumed to be negligible.

7.11 Sub-pixel information for the channel

The subpixel information is available for sensors with higher resolution visible channels in conjunction with lower resolution thermal channels (ABI, AHI, MTG, VIIRS, etc.). For the corresponding IR pixel, the maximum, minimum and standard deviation high resolution pixels are calculated. For the 0.64 μm channel, which has a native resolution of 0.5km for ABI, there are sixteen corresponding pixels that are contained within a single 2km IR pixel.

7.12 Uniformity Tests

7.12.1 Reflectance Uniformity Test (RUT)

The RUT is a daytime test based on the local standard deviation of the observed 0.65 μm reflectance computed for a 3x3 box surrounding each pixel, as calculated by the spatial uniformity algorithm described in the AIADD. If the standard deviation is greater than a threshold, a non-clear result is obtained. The physical basis is the assumption that clear regions should exhibit relatively spatially uniform reflectivity over land and ocean. In an attempt to make the RUT independent of the surface reflectance, the RUT metric is the 0.65 μm reflectance standard deviation over a 3x3 box centered on the current pixel, as computed by the spatial uniformity framework routine described in the AIADD. Because of the non-uniformity of coasts and snow, this test is not applied on those pixels. In the case of RUT and TUT (described below), the standard deviations are always computed using 3x3 pixel arrays. No attempt is made to adjust the resolutions to account for the actual pixel resolution, which is a function of zenith angle. In the ECM, the RUT is applied to the 0.65 μm reflectance standard deviation computed over a 3x3 pixel array for daytime pixels with solar zenith angles out to 80.0 degrees, but can vary depending on the sensor utilized.

As stated above, the goal of the RUT is to separate truly clear pixels from those that are cloud contaminated. An appropriate threshold for the RUT is given by the value for CALIPSO cloud fractions of zero (the most clear of pixels). The initial threshold used is done for each surface type and stored within a given sensor lookup table. In the case of land pixels, however, the threshold is the greater of either 0.5 or the surface index threshold times the clear sky reflectance, as described previously. For water pixels, the RUT has a threshold of that which is stored in the sensor specific lookup table. If the test metric, the standard deviation of the 0.65 μm reflectance standard deviation computed over a 3x3 pixel array for the current pixel is greater than the threshold (the surrounding pixels are non-uniform), then a “true” result is given for the RUT. It is important to note that given the variation along the coast, the RUT is not performed over coastal pixels.

7.12.2 Thermal Uniformity Test (TUT)

The thermal analog to the RUT is the TUT (Thermal Uniformity Test) and is based on the standard deviation of the observed 11 μm brightness temperature computed

on a 3x3 box surrounding each pixel. If the standard deviation is greater than a threshold (the surrounding pixels are non-uniform), a non-clear result is obtained (i.e. test is set to “yes”). Again, because of the fact that coasts are inherently non-uniform, no coast pixels are used in this test. The thresholds used are increased by the value of $3.0 * \Gamma * Z_{\text{std}}$ where Γ is the lapse rate (7.0 K/km) and Z_{std} (km) is the 3x3 standard deviation of the surface elevation. The factor 3 accounts for the fact we are assuming a 3σ departure from the mean elevation. As with the thresholds for the RUT, the TUT thresholds are derived for each sensor and stored with the ECM lookup table.

7.13 Additional Mask Algorithms

The ECM also processes several extra algorithms: Fire, Smoke, Dust, and Thin Cirrus. The results of these products are saved at the compressed bits (Table 5). These additional masks do not affect Cloud Mask and Cloud Probability results and are not validated. The only relevant test is the Thin Cirrus test which is described below.

7.13.1 Thin Cirrus Mask

The Thin Cirrus bit was requested by ECM users (aerosol, land teams, etc.). It works only during the day time, and follows the VCM logic. If $1.38 \mu\text{m}$ reflectance is within minimum and maximum thresholds the Thin Cirrus flag is set to 1. For desert and snow/ice covered pixels the thresholds are different than for the other surfaces.

8 Algorithm Output

The following section describes the four sets of output from the ECM algorithm. The table below shows how the output compares to the Baseline Cloud Mask, and older versions of the ECM, which are both stored in CLASS. For those ATBDs, please refer to the appropriate version of the baseline or enterprise ATBDs.

	Baseline	ECM JPSS v1r0 - v2r4	ECM (JPSS post v2r4, ABI post enterprise update)
Cloud Probability		✓	✓
Binary Mask	✓	✓	✓
4-Level Mask	✓	✓	✓
Packed Test Output	✓	✓	✓

RUT	✓		✓
TUT	✓		✓
VCM Thin Cirrus		✓	✓
Glint	✓	✓	✓

8.1 Cloud Probability Output

The main output of ECM is the Cloud Probability, which is ranging from 0.0 for clear to 1.0 for cloudy. The users are encouraged to use this output for their applications by choosing appropriate thresholds.

8.2 Cloud Mask Output

The ECM consists of a 4-level cloud mask. The cloud mask values and a description of their meaning are given below in Table 4a. Table 4b provides the probabilities for each surface type. The initial value for the ECM is -128.

Table 7 *Cloud mask values and their descriptions*

Cloud Mask Value	Numerical Value
Clear	0
Probably Clear	1
Probably Cloudy	2
Cloudy	3

8.3 Single Classifier Binary Cloud Mask Bits

The algorithm also produces 7 bytes (Table 5) of output which are comprised of bits holding the test results for each of the various tests and flags that are used to compute the cloud probability (0.0 – 1.0) and final 4-level cloud mask product (Table 4), and are required inputs for other algorithms. The first 21 bits, which describe parameters such as

surface type and tests such as the thin cirrus, fire and smoke tests remain static no matter the sensor. The remaining bits are ordered as described in order listed the global attribute for each file.

Table 8 Cloud mask tests and flags and their descriptions.

Flag number	Number of bits	Bits	Byte value	Name
1	1	1	1	Cloud Mask Attempted
2	1	2	1	day flag for 0.63 um refl gross test
3	1	3	1	day flag for 0.63 um spatial gross test
4	1	4	1	3.7 Day Pixel
5	1	5	1	3.7 Night pixel
6	1	6	1	Solar Contamination
7	1	7	1	Coastal Pixel
8	1	8	1	Mountain Pixel
9	1	9	2	Forward Scattering
10	1	10	2	Snow pixel
11	1	11	2	Cold Scene
12	1	12	2	Glint Pixel
13	1	13	2	NB Smoke Flag
14	1	14	2	NB Dust Flag
15	1	15	2	Shadow (not filled)
16	1	16	2	NB Fire Pixel
17	3	17-19	3	ECM Surface Type
18	1	20	3	Thin Cirrus Flag
19	1	21	3	ABI Use of 10.4

All of the 1-bit variables are either 0 = no or 1= yes. The surface type is the surface type used by the naive bayesian mask and is described in section 3.1.4.3. One can pull the surface type using the following bit pattern

001 = Deep Ocean
010 = Shallow Water
011 = Land
100 = Snow
101 = Arctic
110 = Antarctic + Greenland
111 = Desert

The smoke, dust, shadow, fire and thin cirrus bits are added as an extra to the ECM and are not validated. Within the GOES-R Ground System and VIIRS operational processing system, the shadow mask is calculated and stored in the Cloud Height algorithm output files, meaning the bit assigned to the shadow mask is not filled in the packed bits variable.

Because the actual tests used by the ECM are dynamic with each sensor, one must first pull the classifier name attribute from the packed bit variable in order to access the results. Below is a logic to how to access the list of packed bits and extract them, with example code shown in Appendix B. Note that the exact name of the variable from the NDE processing system (SAPF) is **not** the same as what will be contained in the GOES-R Ground System Output or any other processing system the ECM will have different variable and attribute names.

- Read in the packed bits variable (CloudMaskPacked)
- Read in the test names, which are an attribute of the (ECM_test_bit_order)
 - An example of this is shown in Appendix B
- Extract bits based on the position of the classifier (test) in the list of names.
 - The first 21 bits (static_bits) are static (look at the table above).
 - Each test is 1 bit. It is important to remember that IDL is **0 based**. This means the first test would be n=0, the second would be n=1, etc.
 - In the case of output from NDE and CLAVR-x, the packed bits are stored as (byte, x, y).
 - And example from IDL of how to read *a test*, once you know which test (0..n-1) you want to read in, from NDE/CLAVR-x

```

byte_num = fix((static_bits + i) / 8)
test_bit = fix((static_bits + i) - (byte_num* 8))
bit_test = 1

test_output = reform(bit_2_int(fix(packed_tests[byte_num,*,*])), test_bit, bit_test), nelements, nlines, /overwrite)

```

Where packed_tests is the array of packed tests, n is the number which test is, nelements is the number of elements of the array and nlines is the number of lines of the array.

- The packed bits within the GOES-R Ground System are stored within a single (x,y) array, but are only available within the ECM Intermediate product and are not available publicly at this time.

8.4 RUT and TUT

The enterprise cloud mask, like the ABI Baseline Cloud Mask, has two clear-sky uniformity tests which act as filters of the clear pixels to identify clear pixels that reside in regions of high spatial heterogeneity and reclassify them as probably clear. These two tests, which are not part of the actual derivation of the 4-level cloud mask, are available as separate variables for users to utilize if they wish to have an additional reclassification. This reclassification would occur after the pixel is determined to be clear. The typical manner of usage is if the pixel is clear and either of the uniformity tests has a positive result, then the 4-level cloud mask for that pixel is set to “probably clear.” Otherwise, the pixel remains “clear”. The assumption is that the presence of cloud will increase the local spatial heterogeneity beyond the values expected for clear sky.

8.5 Metadata

In addition to the algorithm output and quality flags, the following will be output to the file as metadata for each file for the GOES-R and NDE operational systems:

- Percent of pixels that are clear, probably clear, probably cloudy, and cloudy
- Number of cloud mask categories (4 cloud mask categories: Clear, Probably Clear, Probably Cloudy and Cloudy)
- For each cloud mask category, the following information is required:
 - Count of pixels for the cloud mask category
 - Definition of cloud mask category
- Total number of cloud mask points.
- Terminator mark or determination.
- Minimum, Maximum and Mean observation-calculation for all-sky (IR Channels).

- Minimum, Maximum and Mean observation-calculation for clear-sky (IR Channels).
- Standard deviation between observation and calculation for all-sky (IR Channels).
- Standard deviation between observation and calculation for clear-sky (IR Channels).
- Degraded Scene for FPT event (GOES-R only)

9 Data Sets and Validation Tools

9.1 Input Datasets

This section will describe the datasets used to validate the ECM. The Enterprise Cloud mask currently runs on the VIIRS, ABI, AHI, MODIS and SEVIRI sensors. Future sensors, such as MetImage on EPS-SG, as well as those on Meteosat Third Generation. An example from the ECM as applied to VIIRS and ABI, which are the sensors on the current set of operational United States low-earth orbiting and geostationary satellites.

Figure 11 shows ECM as applied to VIIRS as shown in the figure below, which is an aggregated image from 2030 UTC to 2040 UTC on June 01, 2015. On the left it is a true color image of Hurricane Andres, and on the right – the corresponding 4-level ECM result.

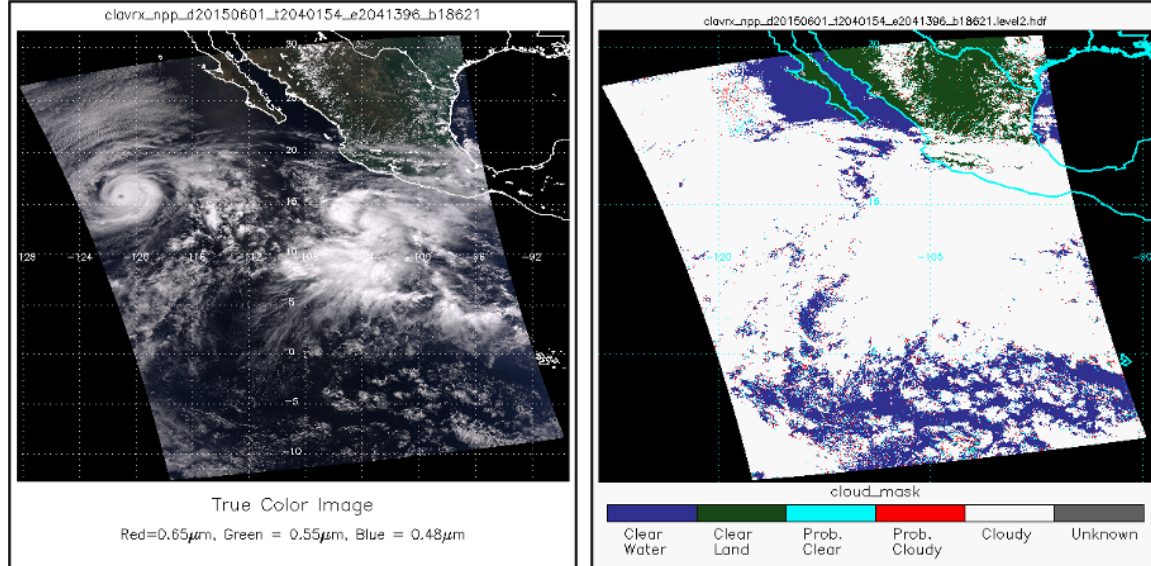


Figure 11 Aggregated images of 8 SNPP VIIRS granules of Hurricane Andres on 06/01/2015 from 2030UTC to 2040UTC (left - True Color RGB, right - NOAA Enterprise Cloud Mask).

VIIRS provides 16 M-Band spectral channels with a nadir spatial resolution of 750 m. It also provides 5 high resolution (375m) bands, with the 0.65 μ m channel being used by the ECM to provide sub-pixel information used as one of the classifiers.

Both the Advanced Himawari Imager (AHI), on JMA's Himawari-8/9 satellites and the Advanced Baseline Imager (ABI), on the GOES-R series of satellites, have 16 bands with the spatial resolution from 0.5 to 2 km. Like VIIRS, this means that the ECM can utilize the sub-pixel information of the high resolution 0.65 μ m channel as one of the classifiers to determine cloud probability. Figure 12 shows an example of GOES-16 ABI Full Disk RGB and ECM from 20 September 2020.

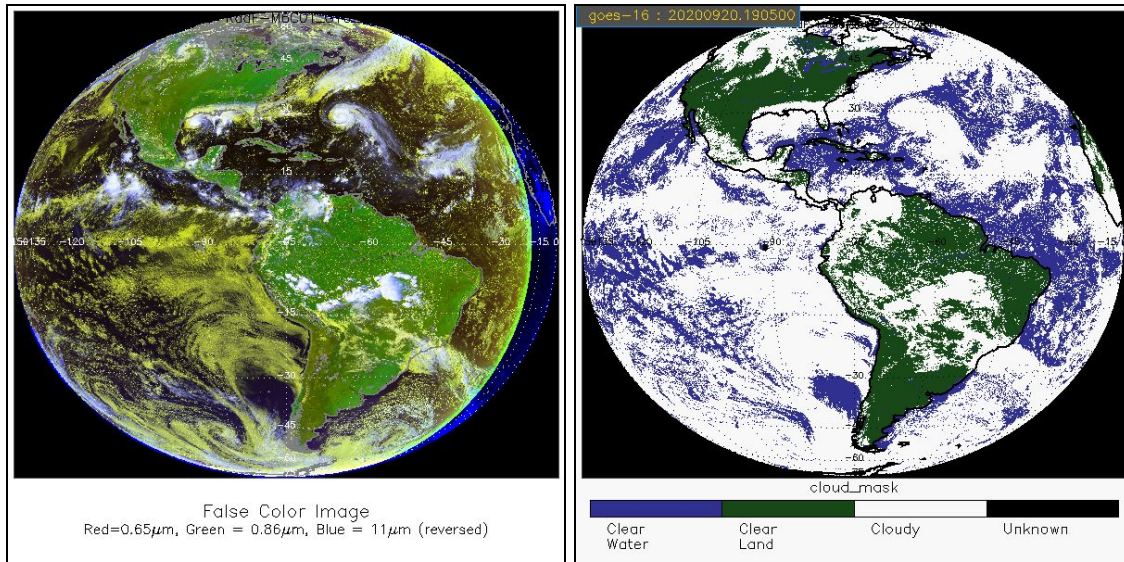


Figure 12 Full Disk GOES-16 ABI RGB and Binary ECM. 2020-09-20 19:00 UTC.

The ECM observations are collocated with CALIPSO data to assess the quality of the ECM performance. These validation data sets are used in assessing the performance of the ECM. In addition, the ECM from VIIRS and ABI can be “warped” to perform inter-sensor consistency.

10 Performance Estimates

This section will provide the performance estimates of the ECM for several of the sensors it is applied to. The estimates will come from application of the CALIOP data designated for testing, which is separated from the data used for training. The

requirements are shown in Table 1. The specifications also say that clouds with optical depths less than 0.4 can be ignored. In showing the performance we do show the ACC metric with COD limitation but we also show the performance without the optical specification. In general, the ECM meets these specifications with any COD limitation.

10.1 ECM Training and Testing Data from Matchups with CALIPSO/CALIOP

With the launch of CALIPSO and CloudSat into the Earth Observing System (EOS) A-Train in April 2006, the ability to conduct global satellite cloud product validation increased significantly. Currently, CALIPSO cloud detection results are used to train and validate the cloud detection of the ECM. The CALIPSO data used here are the 1 km cloud layer results (Vaughan et al., 2005). As with the PATMOS-x cloud mask (Heidinger, et al. 2012), the NASA CALIPSO/CALIOP Cloud Layer Products (CLAY) are used to train the cloud mask. The primary data used are the 5km and 1km CLAY. Both of these are matched in space and time to the satellite pixels. The primary data is the 5km CLAY. For satellite pixels where the 5km CLAY shows no cloud but the 1km CLAY shows cloud, the 1km CLAY values are used. The CLAY products used here are the cloud phase at the top of the highest cloud layer and the integrated cloud optical depth. The 1km CLAY product does not provide cloud optical depth so it is assumed that the cloud detected in the 1km products are optically thick and the cloud optical depth is set to 3. The CLAY cloud phase has 4 values including clear, ice, water and horizontally-oriented ice. The two ice phase categories are counted as a single ice phase.

As discussed in Heidinger et al. (2016), the CALIOP CLAY data has an across-track resolution of 0.333 km and a along-track resolution of 1 and 5km (as used here). The maximum time-difference for sensor collocation was set to +/- 5 minutes. Being a micro-pulsed lidar (MPL), CALIOP is very sensitive to the presence of clouds. To avoid the labelling of pixels as cloudy which have amounts of cloud that are likely invisible to the satellite imagers, CALIOP cloud phases were reclassified as clear if the CALIOP column optical depth was below a threshold. Currently, this threshold is set to 0.1. The ECM training data is generated by using the colocation process and extracting all of the ECM input data along the CALIPSO track and store a file with all of the CALIPSO/CALIOP information. For each sensor, at least one year of data is sampled to generate millions of colocation data. The data is separated into training and testing data by sampling complete days. Typically, the training data is 3 times larger than the testing data.

CALIPSO/CALIOP offers a uniquely high spatial resolution and sensitive data set for training and validating the ECM. However, there are limitations. First, the spatial and temporal differences limit the ability to accurately characterize small scale clouds and cloud edges. Also, CALIPSO is in a sun-synchronous orbit and therefore does not sample all viewing conditions seen by the sensors used in the ECM.

10.2 Performance Metrics

The ECM has always been measured by the Proportional Correct (PC) metric which is also commonly called the accuracy metric (ACC). The number of clouds in the truth data is referred to as P (for positive or yes) and the number of true clear pixels is referred as N (for negative or no). The true positive number (TP) is the number clouds detected correctly and the true negative number (TN) is the number of clear pixels detected correctly. The true positive rate (TPR) is the TP divided by P and the true negative rate (TNR) is the TN divided by N. With these definitions, the ACC metric is computed as

$$ACC = (TP + TN) / (P + N).$$

The cloud fraction of the earth is significantly above 50% and the ACC metric will be driven more by the cloud performance relative to the clear performance. To improve on this, one can derive a balanced accuracy (BACC) metric as

$$BACC = (TP + TN) / 2$$

which balances the clear and cloudy performance.

In addition, these metrics treat the mask as a binary entity. One could bring in the cloud probability values and measure the deviations of the probabilities from 0.0 for clear pixels and 1.0 for cloudy pixels. These metrics would be weighted by these deviations and would penalize the occurrence of “probably” clear and cloudy results and reward confident clear and cloudy results. In these computations, p is the cloud probability which is a floating point number ranging from 0 to 1 and t is the truth probability which only has values of 0 or 1.

With this , the weight ACC metric (WACC) is computed as

$$WACC = 1.0 - \text{mean}((1-t)*p + t*(1-p))$$

and the balanced weighted accuracy metric (BWACC) is computed as

$$BWACC = 1.0 - \text{mean}((1-t)*p*N + t*(1-p)*P) / (N + P)$$

Note, BACC is similar to binary cross entropy (BCE) which is often used in optimizing machine learning approaches.

$$BCE = \text{mean}(-t*\text{alog}(p) - (1-t)*\text{alog}(1-p))$$

In summary, the ECM will report the ACC metric for its validation and use the BWACC metric for its optimization. These other metrics are computed and will also be monitored.

This section will provide the performance estimates of the ECM for several of the sensors it is applied to. The estimates will come from application of the CALIOP data designated for testing, which is separated from the data used for training. The requirements are shown in Table X. The specifications also say that clouds with optical depths less than 0.4 can be ignored. In showing the performance we do show the ACC metric with COD limitation but we also show the performance without the optical specification. In general, the ECM meets these specifications with any COD limitation.

10.3 Estimation of ECM Performance with CALIPSO/CALIOP

As stated above, the ECM performance is based on the ACC metric where clouds with optical depths less than 0.4 are ignored. The performance degrades when the cloud optical depth filter is lessened. In addition, the BACC metric tends to be lower than the ACC metric for a given optical depth filter due to the unbalanced distribution of clouds. Therefore, in addition to the ACC with COD > 0.4 tables, this section will show the BACC tables with no cloud optical depth restriction.

10.3.1 VIIRS Performance Tables

The current VIIRS ECM LUT consists of 18 Classifiers optimized for each surface type. These are listed in Table X used to explain the optimization. Table X provides the breakdown of the VIIRS ECM LUT for each surface type. The table shows the performance in terms of the Performance Metric (PM) and the comparison of cloud fractions between the ECM EF and the truth (TF) which comes from CALIOP. In Table X, the PM is the ACC metric. Table X shows that all surface types exceed the required specification except for the Arctic and Antarctic at night. In general, the EF values are slightly lower than the TF values which indicates the ECM would miss more cloud than it falsely detects. There are exceptions to this as seen in the nighttime results for Antarctica where the EF cloud fraction is 7% higher than the TF value.

Table 9 Performance Metric and Cloud Fraction Comparison for the ECM compared to CALIOP. Performance Metric (PM) is ACC and clouds with optical depths less than 0.4 are ignored. TF is the truth cloud fraction from CALIOP and EF is the cloud fraction from ECM. All refers to all times of day. Day refers to daytime conditions and night refers to nighttime conditions.

surface	All			Day			Night		
	PM	TF	EF	PM	TF	EF	PM	TF	EF
all	0.93	0.70	0.69	0.94	0.70	0.70	0.92	0.71	0.70

deep ocean	0.95	0.78	0.75	0.96	0.74	0.74	0.95	0.83	0.80
other water	0.96	0.79	0.77	0.95	0.78	0.78	0.96	0.81	0.78
land	0.91	0.65	0.61	0.92	0.71	0.71	0.91	0.58	0.54
snow	0.89	0.69	0.67	0.89	0.72	0.72	0.88	0.67	0.66
arctic	0.88	0.75	0.74	0.91	0.76	0.76	0.83	0.73	0.69
antarctic	0.87	0.58	0.62	0.92	0.58	0.58	0.82	0.58	0.65
desert	0.94	0.27	0.28	0.94	0.33	0.33	0.95	0.22	0.24

Table 10 Performance Metric and Cloud Fraction Comparison for the ECM compared to CALIOP. Performance Metric (PM) is BACC and clouds with no optical depths filter TF is the truth cloud fraction from CALIOP and EF is the cloud fraction from ECM. All refers to all times of day. Day refers to daytime conditions and night refers to nighttime conditions.

	All			Day			Night		
	PM	TF	EF	PM	TF	EF	PM	TF	EF
surface									
all	0.90	0.69	0.67	0.92	0.69	0.69	0.88	0.69	0.68
deep ocean	0.93	0.77	0.74	0.94	0.73	0.73	0.92	0.81	0.79
other water	0.93	0.79	0.76	0.93	0.78	0.78	0.93	0.80	0.77
land	0.89	0.64	0.60	0.89	0.70	0.70	0.88	0.57	0.53
snow	0.85	0.67	0.65	0.86	0.70	0.70	0.84	0.65	0.64
arctic	0.81	0.73	0.71	0.84	0.75	0.75	0.78	0.70	0.66
antarctic	0.82	0.56	0.58	0.89	0.57	0.57	0.77	0.55	0.58
desert	0.90	0.29	0.29	0.89	0.34	0.34	0.91	0.24	0.26

10.3.2 ABI+AHI ECM Performance Tables

Following the same optimization procedure, an ECM LUT was constructed from training data from CALIOP matchups with the GOES-16/ABI, GOES-17/ABI and HIM8/AHI. To avoid the loop heat pipe issues, only daytime GOES-17 ABI data were used. The same procedure was run as described for VIIRS. This section follows the format of the

above section. Table X shows the performance tables with ACC as the performance metric and a COD > 0.4

Table 11 Performance Metric and Cloud Fraction Comparison for the ECM compared to CALIOP. Performance Metric (PM) is ACC and clouds with optical depths less than 0.4 are ignored. TF is the truth cloud fraction from CALIOP and EF is the cloud fraction from ECM. All refers to all times of day. Day refers to daytime conditions and night refers to nighttime conditions.

	All			Day			Night		
	PM	TF	EF	PM	TF	EF	PM	TF	EF
surface									
all	0.94	0.72	0.70	0.94	0.71	0.71	0.93	0.74	0.73
deep ocean	0.94	0.74	0.73	0.95	0.73	0.73	0.93	0.78	0.77
other water	0.95	0.72	0.71	0.95	0.71	0.71	0.94	0.77	0.77
land	0.93	0.69	0.66	0.93	0.71	0.71	0.92	0.65	0.62
snow	0.92	0.69	0.67	0.92	0.67	0.67	0.92	0.78	0.76
arctic	0.92	0.72	0.71	0.93	0.71	0.71	0.89	0.73	0.70
antarctic	0.93	0.81	0.81	0.94	0.82	0.82	0.91	0.80	0.79
desert	0.93	0.41	0.38	0.93	0.42	0.42	0.93	0.35	0.35

Table 12 Performance Metric and Cloud Fraction Comparison for the ECM compared to CALIOP. Performance Metric (PM) is BACC and clouds with no optical depths filter TF is the truth cloud fraction from CALIOP and EF is the cloud fraction from ECM. All refers to all times of day. Day refers to daytime conditions and night refers to nighttime conditions.

	All			Day			Night		
	PM	TF	EF	PM	TF	EF	PM	TF	EF
surface									
all	0.90	0.71	0.70	0.91	0.71	0.71	0.88	0.73	0.74
deep ocean	0.91	0.74	0.73	0.92	0.73	0.73	0.88	0.77	0.78
other water	0.92	0.72	0.71	0.92	0.71	0.71	0.90	0.76	0.77
land	0.88	0.67	0.64	0.88	0.68	0.68	0.89	0.63	0.60

snow	0.87	0.67	0.65	0.87	0.65	0.65	0.85	0.76	0.76
arctic	0.86	0.70	0.70	0.86	0.69	0.69	0.85	0.71	0.69
antarctic	0.84	0.79	0.80	0.85	0.80	0.80	0.83	0.77	0.78
desert	0.87	0.41	0.38	0.87	0.43	0.43	0.89	0.35	0.37

10.3.3 MODIS Performance Tables

The ECM is also trained on CALIPSO matchus with the AQUA/MODIS sensor. The same process is applied as described above. Tables X and Y show the resulting performance compared to CALIOP for the ACC metric with COD > 0.4 (Table X) and the BACC metric for COD > 0.01. The MODIS performance shows some similar behavior with VIIRS. The cloud fractions are larger than the nighttime values in the Arctic and Antarctic. All specs are met.

Table 13 Performance Metric and Cloud Fraction Comparison for the ECM compared to CALIOP. Performance Metric (PM) is ACC and clouds with optical depths less than 0.4 are ignored. TF is the truth cloud fraction from CALIOP and EF is the cloud fraction from ECM. All refers to all times of day. Day refers to daytime conditions and night refers to nighttime conditions.

	All			Day			Night		
	PM	TF	EF	PM	TF	EF	PM	TF	EF
surface									
all	0.93	0.71	0.72	0.93	0.70	0.70	0.93	0.73	0.75
deep ocean	0.95	0.79	0.78	0.96	0.76	0.76	0.95	0.82	0.83
other water	0.93	0.83	0.84	0.92	0.83	0.83	0.94	0.84	0.85
land	0.93	0.68	0.64	0.91	0.72	0.72	0.95	0.63	0.62
snow	0.88	0.60	0.64	0.89	0.60	0.60	0.88	0.61	0.66
arctic	0.87	0.63	0.67	0.88	0.62	0.62	0.85	0.64	0.68
antarctic	0.88	0.63	0.70	0.89	0.56	0.56	0.88	0.68	0.78
desert	0.95	0.35	0.34	0.94	0.34	0.34	0.96	0.37	0.37

Table 14 Performance Metric and Cloud Fraction Comparison for the ECM compared to CALIOP. Performance Metric (PM) is BACC and clouds with no optical depths filter TF is the truth cloud fraction from CALIOP and EF is the cloud fraction from ECM. All refers to all times of day. Day refers to daytime conditions and night refers to nighttime conditions.

	All			Day			Night		
surface	PM	TF	EF	PM	TF	EF	PM	TF	EF
all	0.89	0.71	0.71	0.90	0.70	0.70	0.87	0.72	0.73
deep ocean	0.92	0.79	0.78	0.95	0.77	0.77	0.89	0.81	0.82
other water	0.85	0.83	0.84	0.84	0.83	0.83	0.86	0.83	0.84
land	0.90	0.67	0.62	0.89	0.71	0.71	0.92	0.62	0.59
snow	0.84	0.60	0.62	0.85	0.59	0.59	0.83	0.61	0.65
arctic	0.82	0.62	0.64	0.84	0.61	0.61	0.80	0.63	0.65
antarctic	0.81	0.61	0.67	0.85	0.56	0.56	0.77	0.65	0.71
desert	0.90	0.36	0.33	0.87	0.35	0.35	0.92	0.37	0.36

The NASA MODIS MYD35 Cloud Mask was also included in the CALIPSO training data. This allows for a comparison of the MYD35 mask in the same way that the ECM was analyzed. Table X shows the performance of the MYD35 using the BACC metric with COD > 0.01. This table can be compared with Table X for the ECM applied to AQUA/MODIS. The results show general similar performance with the ECM slightly better for the globe as a whole. The MYD35 BACC metric is higher than the ECM's for the nighttime ocean. For the other water surface type, MYD35 also beats the ECM. As shown in the prior discussion, MYD35 cloud fractions tend to be lower than CALIPSO and the ECM.

Table 15 Performance Metric and Cloud Fraction Comparison for the NASA MYD35 compared to CALIOP. Performance Metric (PM) is BACC and clouds with no optical depths filter TF is the truth cloud fraction from CALIOP and EF is the cloud fraction from ECM. All refers to all times of day. Day refers to daytime conditions and night refers to nighttime conditions.

	All			Day			Night		
surface	PM	TF	EF	PM	TF	EF	PM	TF	EF
surface									

all	0.88	0.71	0.64	0.89	0.70	0.70	0.87	0.72	0.65
deep ocean	0.94	0.79	0.75	0.94	0.77	0.77	0.94	0.81	0.77
other water	0.89	0.83	0.77	0.90	0.83	0.83	0.87	0.83	0.80
land	0.86	0.67	0.63	0.86	0.71	0.71	0.87	0.62	0.64
snow	0.80	0.60	0.59	0.81	0.59	0.59	0.80	0.61	0.56
arctic	0.76	0.62	0.45	0.80	0.61	0.61	0.70	0.63	0.40
antarctic	0.78	0.61	0.47	0.84	0.56	0.56	0.75	0.65	0.46
desert	0.86	0.36	0.32	0.85	0.35	0.35	0.88	0.37	0.36

10.4 ECM Sensitivity to Optical Depth

Hit rate is defined as the fraction of clouds relative to the true number of clouds detected by the ECM. Figures X-Y show the hit rate as a function of cloud optical depth measured by CALIOP for each surface type including all surfaces combined for the VIIRS, ABI-AHI and MODIS ECM results. These figures all show that for any optical depth value, the hit rate for the ocean surfaces is highest. In general, the hit rate is above 90% for clouds with optical depths larger than one however the desert surface shows some hit rates < 90% for the ABI-AHI ECM and this needs to be investigated. For the smallest optical depths analyzed (0.01), the hit rates fall to 30%, 45% and 35% for VIIRS, ABI-AHI and MODIS respectively.

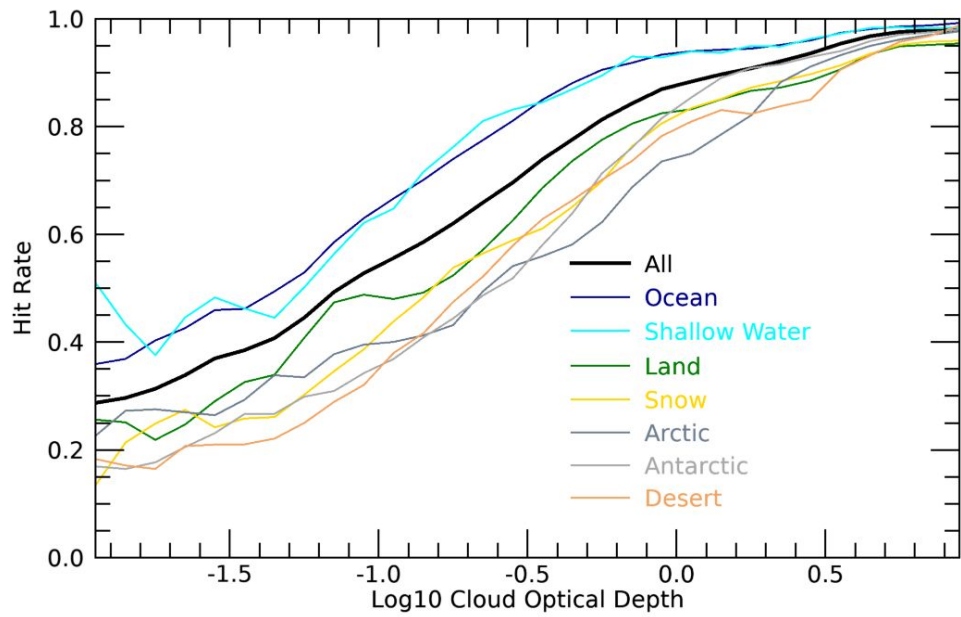


Figure 13 Hit Rate of the ECM as a function of CALIOP Optical Depth. ECM Lut is for VIIRS.

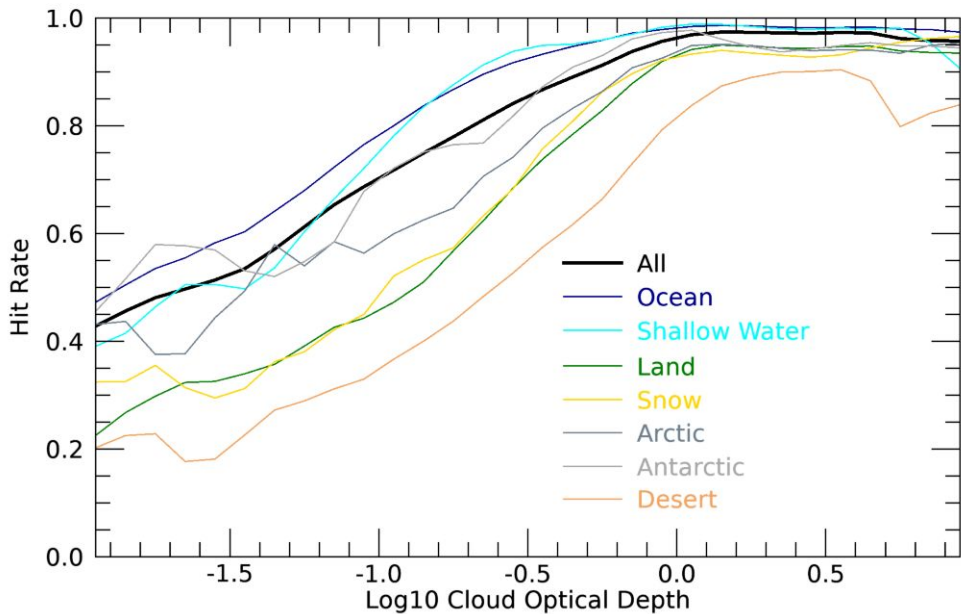


Figure 14 Hit Rate of the ECM as a function of CALIOP Optical Depth. ECM Lut is for ABI/AHI.

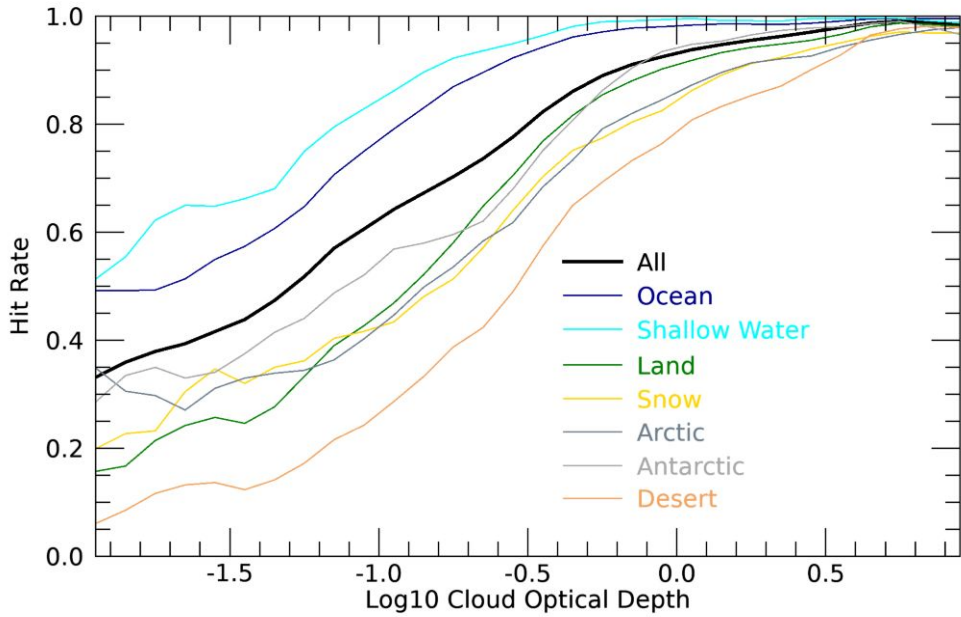


Figure 15 Hit Rate of the ECM as a function of CALIOP Optical Depth. ECM Lut is for MODIS.

One can estimate the optical sensitivity of a cloud detection algorithm by noting the optical depth value where the Hit Rate drops to 50% which means only half of the clouds were detected. If one looks at Figures X-Y, one can estimate the optical depth sensitivity of the ECM to be 0.1, 0.06 and 0.03 for VIIRS, ABI-AHI and MODIS respectively. This pattern of optical depth sensitivity is likely driven by the absence of IR absorption channels on VIIRS. The difference between ABI-AHI and MODIS may be due to difference in spatial coverage and the cloud regimes encountered by these sensors. While not part of the ECM specification, Hit Rates provide a useful to gauge the improvement of the ECM as new classifiers, channels and sensors are

10.5 Intersensor Comparisons

The idea of an enterprise algorithm is that the performance will be similar between satellites. As previously mentioned, the tests that are used are not necessarily the same between satellites, as the lookup tables are optimized for a given sensor. In order to gauge the consistency among sensors, a tool was developed to compare the cloud mask between the ABI/AHI sensors and LEO sensors, such as VIIRS. In order to do this, one needs to first warp the ABI data into the VIIRS granule. This is done by utilizing the reverse geolocation algorithms for a given sensor. In the case of GOES-R, this is described in the GOES-R Product Users guide, while for Himawari they are described in the CGMS LRIT/HRIT Global Specification (2013). This converts the latitude/longitude for the VIIRS granules into the line and elements on the ABI/AHI full disk. In addition, data

taken with as small of a latency between the VIIRS granule and the ABI/AHI scan time. Figure XX shows an example of a NOAA-20 VIIRS ECM granule that is warped into the GOES-16 ABI full disk domain from 2020-09-20 19:00 UTC. As can be seen in the images below, the two cloud masks correspond very closely to each other. There are differences between the two masks, which is to be expected given the resolution differences and some sensor to sensor differences in the classifiers and tests used. Most of the differences occur along the cloud edges and popcorn looking cumulus over the ocean (cyan, red color), which is to be expected due to the spatial resolution difference between the two satellites..

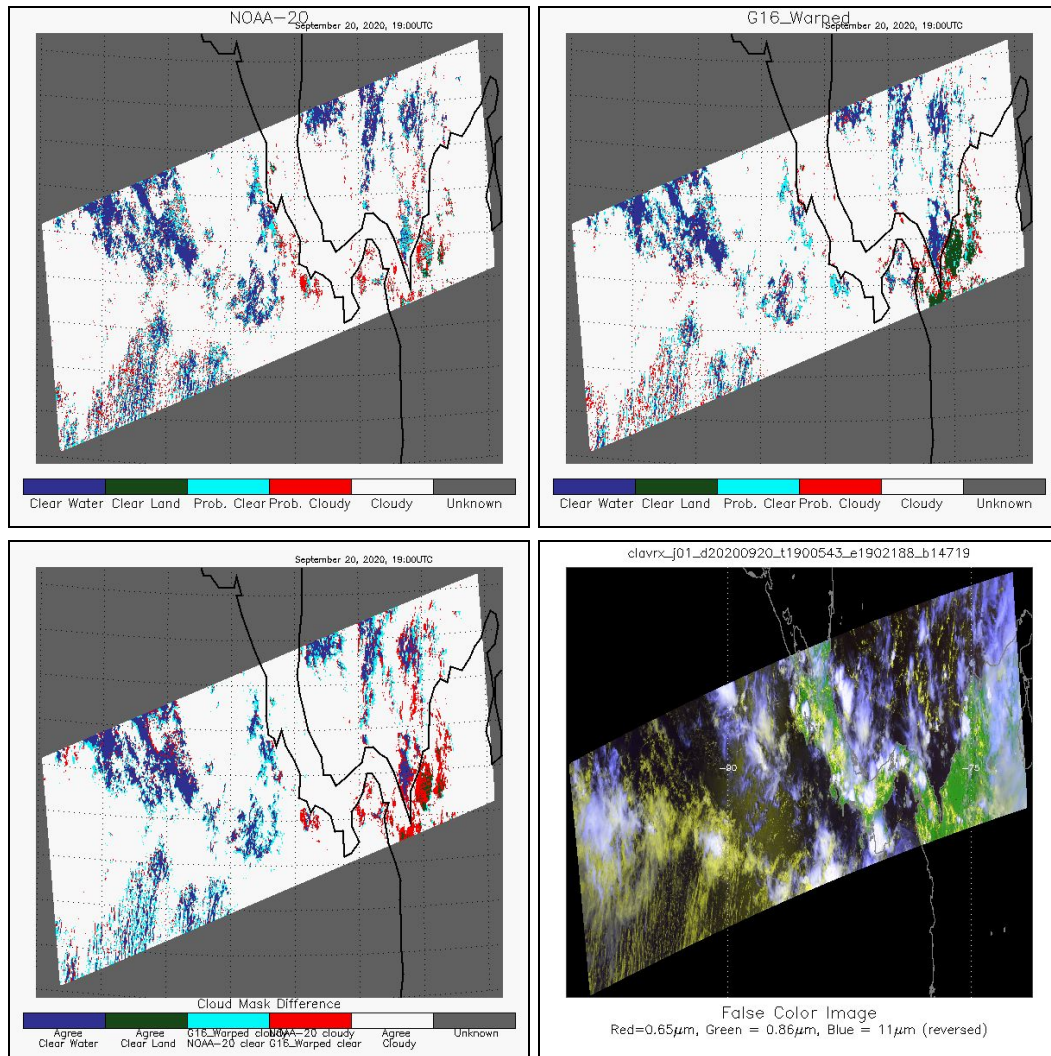


Figure 16NOAA-20 VIIRS ECM, GOES-16 ABI ECM warped to the Leo projection, ECM difference, RGB. 2020-09-20 19:00 UTC

Another way to assess the performance of ECM is to calculate a confusion matrix. The following matrix (Table XX) is calculated for SNPP VIIRS and GOES-16 ABI warped data for 2020-09-20. Both ECM masks are treated as binary (clear for confidently/probably clear, and cloudy if pixels are confidently/probably cloudy). Data is global for any surface and time of day. Overall ECM for both satellites correctly detects clear and cloudy pixels in 87.85% of cases. Situations when ECM VIIRS says clear, and ECM ABI - cloudy is 7.37% of cases, and ECM VIIRS - cloudy, CALIOP - clear is 4.77% cases.

Table 16 Confusion matrix for SNPP VIIRS and GOES-16 ABI global colocation data for 2020-09-20 all surfaces day and night.

		ECM ABI	
		Clear	Cloudy
ECM VIIRS	Clear	182 106 488 (21.57%)	62 285 311 (7.37%)
	Cloudy	40 325 099 (4.77%)	559 550 070 (66.28%)

11 Practical Considerations

11.1 Numerical Computation Considerations

The ECM is implemented sequentially. Because some cloud detection tests rely on the values of the ancillary data flags, the ancillary data flags need to be computed first. All tests are applied before the final cloud mask is determined. The ECM is currently implemented into the Enterprise system and uses its numerical routines for processing.

11.2 Programming and Procedural Considerations

The ECM requires knowledge of spatial uniformity metrics that are computed for each pixel using pixels that surround it. Beyond this reliance, the ECM is purely a pixel by pixel algorithm.

11.3 Quality Assessment and Diagnostics

The following procedures are recommended for diagnosing the performance of the ECM.

- Monitor the percentage of pixels falling into each ECM cloud mask value. These values should be quasi-constant over a large area.
- Periodically image the individual test results to look for artifacts or non-physical behaviors.

- Maintain a close collaboration with the other teams using the ECM in their product generation.

There is some routine monitoring done by the NOAA Cloud team via a website, however operationally monitoring of the ECM is performed by OSPO and focuses on the monitoring of percentage of pixels falling into each ECM cloud mask value (clear, prob. clear, prob. cloudy, cloudy). The Cloud team website, which is not an operational monitoring system, has multiple aspects to it. This includes imaging of all the cloud products as well as RGBs as well as trend analysis of the various products. The routine imaging helps in verifying that the products are being produced in a correct manner (i.e. there are no angle issues in the processing system). The trend analysis serves multiple purposes. The first is to ensure that the products are producing data within the expected range and identification of issues. Any deviation outside the expected norm can be used by the Cloud team to identify any potential ground system issues. It is important to note, again, that the ground systems have their own operational tools which should alert them to such issues, but this can serve as a method for the team to identify subtle issues and impacts (ex. calibration issues on VIIRS). The second is that the monthly composites and comparisons can show if the sensors, particularly VIIRS, are performing in a similar manner (i.e. do SNPP and NOAA20 have the same cloud distribution). Finally, the trends can serve as a method of identifying if new LUTs are implemented correctly within the ground system and are performing as expected (ex. verifying the change between JPSS v2r2 and v2r3 had a correction to reduce overclouding over snow).

11.4 Exception Handling

The ECM includes checking the validity of each channel before applying the appropriate test. The ECM also expects the main processing system (i.e., the Enterprise) to flag any pixels with missing geolocation or viewing geometry information.

The ECM does check for conditions where the ECM cannot be performed. If the 11 μm channel measured or clear sky BT is saturated or missing, there is no attempt at processing the cloud mask, as it is a key channel in numerous tests for the ECM. If other channels are saturated or missing, the corresponding tests are not performed. A quality flag is set, which indicates the quality of the cloud mask for that particular pixel. The conditions for the quality flags are described in Section 3.4.2.2.

12 ASSUMPTIONS AND LIMITATIONS

The following sections describe the current limitations and assumptions in the current version of the ECM.

12.1 Performance

The following assumptions have been made in developing and estimating the performance of the ECM. The following list contains the current assumptions and proposed mitigation strategies.

1. NWP data of comparable or superior quality to the current 6 hourly GFS forecasts are available. (Use longer range GFS forecasts or switch to another NWP source – ECMWF).
2. RTM calculations are available for each pixel. (Use reduced vertical or spatial resolution in driving the RTM).
3. High quality snow maps are available. (Use snow information from NWP).
4. Background snow-free surface reflectances will be available. (Use precomputed reflectances stored as function of surface type).
5. All of the static ancillary data is available at the pixel level. (Reduce the spatial resolution of the surface type, land mask and or coast mask).

12.2 Assumed Sensor Performance

The ECM is dependent on the following instrumental characteristics:

- The spatial uniformity tests in ECM will be critically dependent on the amount of striping in the data.
- Unknown spectral shifts in some channels will cause biases in the clear-sky RTM calculations that may impact the performance of the ECM.

12.2.1 Planned Product Improvements

The Naive Bayesian (NB) method employed here is part of a library of machine learning (ML) methods. Experience has shown that there are superior ML methods for this application. Our plans are to switch out the NB method in favor of other methods including Neural Network (NN) and other Artificial Intelligence (AI) approaches.

In addition, the ECM also provides cloud phase information used in support of other ECM applications. We are studying if this information is helpful to users in diagnosing cloud detection issues and if successful, this information may make its way in the official ECM output.

The ECM is very much tied to its downstream applications and future improvements will be driven by their needs.

12.2.2 Optimization for Applications

The ECM performance over land also needs to be optimized for the other Enterprise Algorithms which rely on clear-sky detection. For example, coordination with the Land and Cryosphere Application Teams regarding the ECM algorithm and output is being done to allow for their feedback and to ensure the ECM is adequate for their needs.

13 REFERENCES

- Ackerman, S.A., K.I. Strabala, W.P. Menzel, R.A. Frey, C.C. Moeller and L.E. Gumley, 1998: Discriminating clear sky from clouds with MODIS. *J. Geophys. Res.*, **103**, 32139-32140.
- Ackerman, S. A., Strabala, K. I., Menzel, W. P., Frey, R. A., Moeller, C. C., Gumley, L. E., Baum, B., Wetzel-Seeman, S., and Zhang, H.: Discriminating clear sky from clouds with MODIS Algorithm Theoretical Basis Document (MOD35), Tech. Rep. ATBD-MOD-06, University of Wisconsin-Madison, 2002
- Baglio, J.V., and Holroyd, E.W., 1989. Methods for operational snow cover area mapping using the advanced very high resolution radiometer: San Juan Mountains Test Study, Research Technical Report, U.S. Geological Survey, Sioux Falls and U.S. Bureau of Reclamation, Denver.
- Derrien M., and H. Le Gleau, MSG/SEVIRI cloud mask and type from SAFNWC, International Journal of Remote Sensing 26 (2005), pp. 4707–4732.
- Dozier, J., 1989. "Remote sensing of snow in visible and near-infrared wavelengths," Theory and Applications of Optical Remote Sensing, G. Asrar, ed., John Wiley and Sons, New York.
- Dybbroe, A., K.G. Karlsson, and A. Thoss, 2005: NWCSAF AVHRR Cloud Detection and Analysis Using Dynamic Thresholds and Radiative Transfer Modeling. Part I: Algorithm Description. *J. Appl. Meteor.*, **44**, 39–54.

Dybbroe, A., K.G. Karlsson, and A. Thoss, 2005: NWCSAF AVHRR Cloud Detection and Analysis Using Dynamic Thresholds and Radiative Transfer Modeling. Part II: Tuning and Validation. *J. Appl. Meteor.*, **44**, 55–71.

GOES-R Series Ground Segment (GS) Project Functional and Performance Specification (F&PS) [G417-R-FPS-0089]

GOES-R Level 1 Requirements Document (L1RD)

GOES-R Series Mission Requirements Document (MRD) [P417-R-MRD-0070]

GOES-R Acronym and Glossary (P417-R-LIST-0142)

GOES-R Algorithm Interface and Ancillary Data Description Document (AIADD)

Hann, S.L.L. Strow, and W.W. McMillan, 1996: Atmospheric infrared fast transmittance models: A comparison of two approaches, Proceedings of SPIE, 2830, 94-105.

Hansen, M., R. DeFries, J.R.G. Townshend, and R. Sohlberg (1998), UMD Global Land Cover Classification, 1 Kilometer, 1.0, Department of Geography, University of Maryland, College Park, Maryland, 1981-1994.

Heidinger, Andrew K.; Evan, Amato T.; Foster, Michael J. and Walther, Andi.: A naive Bayesian cloud-detection scheme derived from CALIPSO and applied within PATMOS-x. *Journal of Applied Meteorology and Climatology*, Volume 51, Issue 6, 2012, 1129–1144

Heidinger, Andrew K.; Frey, Richard and Pavolonis, Michael.: Relative merits of the 1.6 and 3.75 micron channels of the AVHRR/3 for cloud detection. *Canadian Journal of Remote Sensing*, Volume 30, Issue 2, 2004, pp.182-194.

Hunt, G. E., 1973: Radiative properties of terrestrial clouds at visible and infrared thermal window wavelengths. *Quart. J. Roy. Meteor. Soc.*, 99, 346–369.

Inoue, T., 1985: On the temperature and effective emissivity determination of semi-transparent clouds by bi-spectral measurements in the 10 micron window region. *J. Meteor. Soc. Japan*, 63 (1), 88–89.

Inoue, T., 1987: A cloud type classification with NOAA 7 split window measurements. *J. Geophys. Res.*, 92, 3991-4000.

Joint Polar Satellite System (JPSS) Level 1 Requirements Document (L1RD), Version 1.8, June 25, 2014

Joint Polar Satellite System (JPSS) Program Level 1 Requirements SUPPLEMENT (L1RDS), Version 2.10, June 25, 2014

Joint Polar Satellite System (JPSS) Operational Algorithm Description (OAD) Document for VIIRS Cloud Mask (VCM) Intermediate Product (IP) Software

Joint Polar Satellite System (JPSS) VIIRS Cloud Mask (VCM) Algorithm Theoretical Basis Document (ATBD)

Joro S., Samain O., Yildirim A., van de Berg L., Lutz H.J.: Towards an improved active fire monitoring product for MSG satellites. 2008.

http://www.eumetsat.int/Home/Main/AboutEUMETSAT/Publications/ConferenceandWorkshopProceedings/2008/SP_1232700911980

Kopp, Thomas J.; Thomas, W.; Heidinger, Andrew K.; Botambekov, Denis; Frey, Richard A.; Hutchison, Keith D.; Iisager, Barbara D.; Brueske, Kurt; and Reed, Bonnie; The VIIRS Cloud Mask: Progress in the first year of S-NPP toward a common cloud detection scheme. Journal of Geophysical Research - Special Issue of the Suomi National Polar-Orbiting Partnership Satellite Calibration, Validation and Applications, Volume 118, 2013, pp. SNPP403 - SNPP418, doi:10.1002/2013JD020458.

Krebs, W., Mannstein, H., Bugliaro, L., and Mayer, B.: Technical note: A new day-and night-time Meteosat Second Generation Cirrus Detection Algorithm MeCiDA, Atmos. Chem. Phys., 7, 6145-6159, doi:10.5194/acp-7-6145-2007, 2007.

LRIT/HRIT Global Specification, CGMS, 2013
http://www.cgms-info.org/index_.php/cgms/page?cat=PUBLICATIONS&page=Technical+Publications

Li, J. and K. Shibata, 2006: [On the Effective Solar Pathlength](#). Journal of the Atmospheric Sciences 2006 63:4, 1365-1373

Moody, E.G., M.D. King, C.B. Schaaf, and S. Platnick, 2008: MODIS-Derived Spatially Complete Surface Albedo Products: Spatial and Temporal Pixel Distribution and Zonal Averages. J. Appl. Meteor. Climatol., 47, 2879–2894.

Pavolonis, M. J., 2009: Advances in extracting cloud composition information from spaceborne infrared radiances: A robust alternative to brightness temperatures. Part II: Proof of concept. Submitted to *J. Atmos. Sci.*

Prabhakara, C., R. S. Fraser, G. Dalu, M. C. Wu, and R. J. Curran, 1988: Thin cirrus clouds: Seasonal distribution over oceans deduced from Nimbus-4 IRIS. *J. Appl. Meteor.*, 27, 379–399.

Schreiner, Anthony J.; Ackerman, Steven A.; Baum, Bryan A. and Heidinger, Andrew K.: A multispectral technique for detecting low-level cloudiness near sunrise. *Journal of Atmospheric and Oceanic Technology*, Volume 24, Issue 10, 2007, pp.1800-1810.

Seemann, S.W., E. E. Borbas, R. O. Knuteson, G. R. Stephenson, H.-L. Huang, 2007: Development of a Global Infrared Land Surface Emissivity Database for Application to Clear Sky Sounding Retrievals from Multi-spectral Satellite Radiance Measurements. *Journal of Applied Meteorology and Climatology*, accepted April 2007.

Stowe, L.L., P.A. Davis, and E.P. McClain, 1999: Scientific Basis and Initial Evaluation of the CLAVR-1 Global Clear/Cloud Classification Algorithm for the Advanced Very High Resolution Radiometer. *J. Atmos. Oceanic Technol.*, 16, 656–681.

Thomas, Sarah M.; Heidinger, Andrew K. and Pavolonis, Michael J.: Comparison of NOAA's operational AVHRR-derived cloud amount to other satellite-derived cloud climatologies. *Journal of Climate*, Volume 17, Issue 24, 2004, pp.4805-4822.

Vaughan, M. A., Winker, D. M., and Powell, K. A.: CALIOP algorithm theoretical basis document. Part 2: Feature detection and layer properties algorithm, PC-SCI-202, Release 1.01, 87 pp., [http://www-calipso.larc.nasa.gov/resources/project documentation.php](http://www-calipso.larc.nasa.gov/resources/project/documentation.php), 2005.

Wang, M., & King, M. D. (1997). [Correction of Rayleigh scattering effects in cloud optical thickness retrievals](#). *Journal of Geophysical Research-Atmospheres*, 102(D22), 25915-25926

Warren, S., 1982. Optical properties of snow, *Reviews of Geophysics and Space Physics*, 20, 67.

Wu, Xiangqian, W. Paul Menzel, and Gary S. Wade, 1999: Estimation of Sea Surface Temperatures Using GOES-8/9 Radiance Measurements. Bulletin of the American Meteorological Society Volume 80, Issue 6 (June 1999) pp. 1127–1138

14 Appendix A Calculation of Solar Scattering Terms

14.1 Rayleigh Scattering

The Rayleigh or molecular optical scattering is taken from the cloud mask threshold include file and is not computed during execution. We have estimated that the total in-band to 0.63 μm channel Rayleigh optical depth is approximately 0.05. The Rayleigh phase function is used to account for the angular distribution of the Rayleigh scattering.

$$P_{Ray} = 0.75(1 + \mu^2) \quad (1)$$

where μ is the cosine of the scattering angle where scattering angle is defined by the solar and viewing geometries.

14.2 Aerosol Scattering

To model the aerosol scattering, a Henyey-Greenstein phase function was assumed as illustrated below.

$$P_{aer} = \frac{(1 - g_{aer}^2)}{\sqrt{(1 + g_{aer}^2 - 2g_{aer}\mu)^3}} \quad (2)$$

In the above equation, g_{aer} is the asymmetry parameter. The single scatter albedo ($\omega_{o,aer}$), g_{aer} and total column aerosol optical depth, τ_{aer} , are provided in the cloud mask threshold include files.

14.3 Gaseous Absorption

The main absorbing gases in the 0.63 μm channel are water vapor and ozone. The total column optical depths (t) are computed using polynomial regressions based on the total precipitable water (TPW) and total column ozone ($TOZONE$).

$$\tau_{H_2O} = a + b(TPW) + c(TPW^2) \quad (3)$$

$$\tau_{O_3} = a + b(TOZONE) + c(TOZONE^2) \quad (4)$$

The coefficients (a , b , c) for the water vapor and ozone optical depth regressions were computed using MODTRAN4 and the assumed 0.63 μm channel spectral response

functions. For use in this routine, the ozone and water vapor optical depths are combined in one gaseous optical depth, τ_{gas} .

$$\tau_{gas} = \tau_{H_2O} + \tau_{O_3} \quad (5)$$

14.4 Computation of Clear-sky Reflectance

The computation of the clear-sky 0.63 μm channel reflectance is done by combining a single scattering approximation coupled with an isotropic two-stream approximation. This formulation is a modified version of that used by the MODIS Atmospheres Science Team and described by Wang and King (1997).

To compute the clear-sky reflectance, several intermediate terms are needed. First, a total optical depth, τ_{total} , is computed from the Rayleigh, aerosol and gas optical depths.

$$\tau_{total} = \tau_{Ray} + \tau_{aer} + \tau_{gas} \quad (6)$$

In addition, a total optical depth for isotropic scattering computed as follows

$$\tau_{isototal} = \tau_{Ray} + (1 - g_{aer})\tau_{aer} + \tau_{gas} \quad (7)$$

where the aerosol optical depth is scaled by $1 - g_{aer}$. The effective single scatter albedo, ω_o , of the entire column is computed as

$$\omega_o = \frac{(\omega_{o,aer}\tau_{aer} + \tau_{ray})}{\tau_{total}} \quad (8)$$

and the effective phase function, P , of the entire column is computed as

$$P = \frac{(\omega_{o,aer}\tau_{aer}P_{aer} + \tau_{Ray}P_{Ray})}{\tau_{scattotal}} \quad (9)$$

where $\tau_{scattotal}$ is the total scattering optical depth.

$$\tau_{scattotal} = \tau_{Ray} + \omega_{o,aer}\tau_{aer} \quad (10)$$

The 0.63 μm channel clear-sky reflectance, $R_{2,clear}$, is computed from three terms. The first term, R_a , accounts for the single scattering contribution of the atmosphere. R_a is computed using the following relation

$$R_a = \left(\frac{\varpi_o P}{(4m\mu_v \mu_o)} \right) (1 - T_{ss}) \quad (11)$$

where m is the airmass factor ($\frac{1}{\mu_v} + \frac{1}{\mu_o}$) is the single-scattering transmission term computed as

$$T_{ss} = e^{-(\tau_{total}/\mu)} \quad (12)$$

The second term, R_b , accounts for the contribution of reflectance scattered in the atmosphere and then scattered off the surface and is computed as follows

$$R_b = \frac{\tau_{isqscattotal}}{(2\mu_o)} T_{iso,total/view} \alpha_{sfc} \quad (13)$$

where α_{sfc} is the surface albedo, and $T_{iso,total/view}$ is the transmission term computed along the viewing direction assuming isotropic scattering.

$$T_{iso,total/view} = e^{-(\tau_{isqtotal}/\mu)} \quad (14)$$

The third term, R_c , is the contribution of reflectance scattered off the surface from the direct solar beam and then scattered in the atmosphere. This term is given by

$$R_c = \frac{\tau_{isqscattotal}}{(2\mu_v)} T_{iso,totalsun} \alpha_{sfc} \quad (15)$$

where

$$T_{iso,totalsun} = e^{-(\tau_{isqtotal}/\mu_o)} \quad (16)$$

The final clear-sky 0.63 μm channel reflectance is computed simply as

$$R_{2,clear} = 100(R_a + R_b + R_c) \quad (17)$$

where the factor converts the reflectance to a percentage.

15 Appendix B. IDL Code to Read Individual Classifier Masks

Below is sample IDL code to access the binary cloud mask from a single classifier from a netcdf file from CLAVR-x. Other processing systems, like SAPF, will be accessed via different variables, but the methodology is similar for each output file.

```
;-----  
; example IDL code to extract the binary cloud mask predicted  
; by each classifier  
;  
; input:  
; file_name = name of netcdf ecm product file  
; class_name = name of an ecm classifier  
; output:  
; classifier_result = the binary cloud mask of the classifier  
;-----  
pro extract_class_mask, file_name, class_name, classifier_result  
  
;--- the number of non-cloud bits at the beginning of the packed bits  
class_idx_offset = 21  
  
;---- names of the classifier data and classifier names attribute  
sds_name = 'cloud_mask_test_packed_results'  
sds_attr_name = 'classifier_names'  
  
;--- open read and close file  
sd_id = ncdf_open(file_name)  
sds_id = ncdf_varid(sd_id, sds_name)  
ncdf_attget, sd_id, sds_id, sds_attr_name, classifier_names_temp  
ncdf_varget, sd_id, sds_name, packed_results  
ncdf_close, sd_id  
  
;--- convert classifier names to a string array  
dummy = strarr(classifier_names_temp.length)  
for i = 0, dummy.length - 1 do dummy[i] = string(classifier_names_temp[i])  
classifier_names = strsplit(strjoin(dummy), ',', /extract)  
  
;--- find where class_name sits in the classifier_names array  
idx = where(class_name eq classifier_names, cc)  
if (idx eq -1) then begin  
    print, 'classifier name not valid'  
    classifier_result = -1  
endif else begin  
  
;--- determine on which byte and bit, this result can be found  
idx_class = class_idx_offset + idx[0]  
class_byte = (idx_class) / 8
```

```
class_bit = idx_class - 8*class_byte  
  
;- extract binary mask for this classifier  
temp = packed_results[class_byte,:,:]  
classifier_result = reform(ishft(ishft(temp,7-class_bit),-7))  
  
endelse  
  
end
```